M. H. HETHERINGTON

PH.D.

1997

This is to certify that the

dissertation entitled

MEASUREMENT OF THE AIR FLOW CHARACTERISTICS OF AGRICULTURAL AIR CARRIER SPRAYERS

presented by

Michael H. Hetherington

has been accepted towards fulfillment
of the requirements for

Ph.D. degree in Ag. Engineering

Major professor

Date 30 April 1997

PLACE IN RETURN BOX to remove this checkout from your record.
TO AVOID FINES return on or before date due.
MAY BE RECALLED with earlier due date if requested.

DATE DUE	DATE DUE	DATE DUE

1/98 c:/CIRC/DateDue.p65-p.14

MEASUREMENT OF THE AIR FLOW CHARACTERISTICS OF AGRICULTURAL AIR CARRIER SPRAYERS

By

Michael H. Hetherington

A DISSERTATION

Submitted to
Michigan State University
in partial fulfillment of the requirements
for the degree of

DOCTOR OF PHILOSOPHY

Department of Agricultural Engineering

1997

ABSTRACT

MEASUREMENT OF THE AIR FLOW CHARACTERISTICS OF AGRICULTURAL AIR CARRIER SPRAYERS

By

Michael H. Hetherington

The measurement of the air velocity field from moving air carrier agricultural chemical application equipment is discussed. A three-dimensional field 2 meters × 3 meters × 3 meters was measured for two conventional radial diffuser, and one tower type sprayer. Pitot tube pressure sensors were used on a pole to measure 15 height locations at four distances from the equipment at a sampling frequency of 1000 Hz. Techniques for analyzing and displaying the recorded data are presented. The resulting data shows characteristics of the flow pattern unique to each type of machine. Mean jet velocity and turbulence number in the field measured are analyzed and displayed. The results of two different towing speeds are also shown.

Dedicated to Patricia Hetherington for her love and support.

ACKNOWLEDGMENTS

Thanks to everyone involved in helping me complete this project, including, but not limited to:

- Dr. Jack Hetherington, for his teaching and assistance in various mathematical issues in this thesis and throughout life.
- Dr. Gary Van Ee, for his guidance, patience and assistance in completing this project.
- Dr. Robert Falco, for providing me with an understanding of fluid dynamics and turbulence.
- Richard Ledebuhr, for his assistance and almost infinite understanding of mechanical processes.

TABLE OF CONTENTS

LIST OF TABLES

LIST OF FIGURES

Chapter 1

INTRODUCTION

1.1 Background

A forced jet of air used to deliver chemicals to a target has been shown to be an effective way to evenly distribute chemicals in addition to directing the chemical toward a specific target area. Examples of equipment that use this principle range from the air powered paint sprayer to the agricultural orchard "air blast" sprayer. The advantage of air carrier chemical application is that it allows the air to carry very fine particles or drops to the target. Fine particles have a very high drift potential, they quickly attain the velocity of the surrounding fluid. This makes small particles difficult to control if they are applied directly, because they will drift wherever the surrounding air currents travel. However, it is easy to direct the particles if the surrounding air stream is controlled.

The basic principle of agricultural air carrier sprayers is that a chemical mixture is released into a relatively high velocity air flow which delivers the chemical to the target. Several factors influence a piece of equipment's effectiveness, these are: 1) droplet size and variation, 2) chemical type, and, 3) air flow characteristics including speed, direction, fluctuation and volume. While the droplet and chemical properties are important, perhaps the single most important variable to application technology is the air flow into which it is released. If the air is to deliver the chemical to the target then the air must be directed at the target. While this sounds very simple, it is difficult to instrument and even harder to implement.

The basic design of most of today's air carrier agricultural sprayers are surprisingly similar to the first machines developed in the 1940's (Michigan State University, Northwest Experiment Station, 1994). In the design of common sprayers, a central axial fan forces air out through a diffuser where chemicals are released into the air stream. This diffuser is usually located near the ground and the air flow is generally upwards in a radial pattern. Recently, some manufacturers have extended the diffusers up into towers which can aim the air directly at taller parts of a tree. Other manufactures have used vertically mounted cross-flow fans to distribute the air flow more evenly across an entire tree canopy. The designs that produce an even distribution of the air appear to control plant diseases more effectively with less chemical (Grafius, et al., 1990) (Derksen and Gray, 1995). For this reason a systematic approach needs to be developed to study the important characteristics of the air flow parameter.

1.2 General Industry Need

There is an obvious need to reduce the amount of chemicals released into the environment. A growing public awareness, serious environmental concerns and simple economics are all demanding better methods of applying chemicals.

Certain parameters are needed for the immediate improvement of air-carrier chemical application. These parameters are, as outlined by Bukovac (1985), "...spray equipment characteristics, spray penetration of the tree canopy, and non-uniform distribution of the spray over the tree."

1.3 Current Practices in Air Flow Measurements

The study of air flows has been a primary issue in many engineering fields, ranging from duct flow in the heating and cooling field to aerodynamic thrust and lift in the airplane industry. Perhaps the largest amount of fluid dynamic and turbulence research has been conducted by the aeronautics field where extremely small improvements in aerodynamic efficiencies have huge economic savings. Entire journals exist about fluid dynamic research: "The Journal of Fluids Engineering," "The Physics of Fluids," "The Journal of Fluid Mechanics," and "The Fluid Measurement Journal" just to name a few. Tremendous efforts and entire careers have been made studying very specific aspects of a flow, such as the flow near a strut and fuselage interface or the nature of turbulent eddies in a boundary layer. These studies have huge budgets, because of the tremendous economic benefits that even a minor improvement would have for the military and commercial aviation industry.

Current practices of airflow measurements in agricultural chemical application are quite limited. The major method of assessing sprayers has been through deposition studies, followed by some correlation to the equipment that produced the best results. While these results may be useful to help rate the currently available air carrier sprayers, they are not very useful for the engineer faced with improving the design of these machines. These studies do not isolate the many parameters of chemical deposition; therefore, it is difficult to determine which parameters actually are responsible for the better performance.

A few studies to measure air flow in sprayers have been performed. Sven Svensson (1991) reports measuring seven points of in-tree air flow using one type of sprayer. Researchers at Wooster Research Station in Ohio performed an experiment on a stationary set of fans to correlate the results with a mathematical model that was being developed (Fox, et al., 1985). These studies have been limited in their instrumentation and scope. Another unpublished study employed the technology of high speed three-dimensional turbulence measurements; unfortunately, the difficulties and cost of obtaining these kinds of measurements led to only a few physical locations of measurement and yielded data which could not be correlated back to the spray units which produced the air flow. This data was never used. The most recent published study by Salyani and Hoffmann (1996) claims that one objective is to “Characterize air velocity profiles of a stationary and traveling air-carrier sprayer.” This study actually measured only peak velocities and made no attempt to account for turbulence or to map the velocity profiles.

The extent to which individual manufacturers are conducting air flow research is undocumented and basically unknown. Examining current production machines leads one to conclude that very little effective research has been done. Numerous examples of poor aerodynamic design can be seen on these machines.

Diffusers and ducts on most sprayers are simple welded plates and do not follow the design parameters of NASA duct standards. With today's fiberglass and thermoplastic manufacturing techniques there is little reason that smoother, and therefore better, ducting design could not be implemented if the benefits of improved aerodynamic design were understood.

The vast amount of information and research regarding air flow, developed by the aviation and other industries, provides a tremendous resource for the chemical application engineer to use for the improvement of sprayer design. Unfortunately, over 80 years of aerodynamic research can be confusing and complicated. Much of the basic research conducted on airplanes in the 1930's has not yet been performed on today's agricultural sprayers. It is tempting to apply modern high-tech aerodynamic experiments to agricultural chemical application, but these techniques may yield erroneous results. Skipping ahead ignores almost 60 years of development that aviation research has enjoyed. The technological developments in measurement instruments, computers and the increased understanding of fluids gives today's engineers a significant advantage over the engineer of 1930. The same type of information gathered for airplanes in the thirties and forties needs to be collected before a systematic approach to improving the air flow and deposition characteristics of air carrier agricultural sprayers can be developed.

1.4 Objectives

The primary goal of this research is to determine an effective means of measuring and evaluating the air flow characteristics of agricultural air carrier sprayers. By developing tools and studying the current equipment the characteristics that are responsible for more efficient and effective chemical application can be determined.

The more specific objective of this thesis is to develop a technique to study the air flow of commercially available sprayers. The scale of the flow that is of primary interest is the delivery of air from the sprayer to the canopy. Developing a measurement system that can provide velocity maps for various machines in actual field environments is necessary to achieve this objective.

Chapter 2

THEORETICAL CONSIDERATIONS AND DETERMINATION OF MEASUREMENT TECHNIQUES BASED ON REVIEW OF PERTINENT LITERATURE

2.1 Introduction

The study of air flow is a broad and vast field. To practically measure a flow field, an understanding of the goals and objectives of the measurements must be determined. Once the goals and objectives have been determined, they can be used to narrow the scope of the study by assisting in making justifiable assumptions and eliminating relatively unimportant parameters. These assumptions will then allow the selection of appropriate measurement and analysis techniques. The ability to determine which parameters are important as well as those that are unimportant is imperative to productive research.

This chapter will explain the major considerations that lead to the measurement and analysis choices for our objectives. While most of the considerations are not unique to our flow fields, the combination of all practical and theoretical considerations makes it impossible to employ a standard measurement technique from another industry, such as aviation or heating and cooling.

The concepts presented in this chapter are basic fluid dynamic and turbulence concepts. Specific references are not always cited, because many of the statements are concepts related by several authors. Many of these concepts were derived from texts by Tennekes and Lumley (1972), Hinze (1959), Batchelor (1953), Potter & Foss (1982), and papers and lectures from Dr. Foss and Dr. Falco of Michigan State University.

2.2 The Transport of Chemical Particles in an Air Flow

Studying air-carrier chemical application requires an understanding of the ability of air to carry the chemical to the target and deposit it once it reaches the target. When small droplets or particles are introduced to an air stream the drag force of the air tends to accelerate them in the direction of the air flow. If the droplet is small enough then the acceleration of the drag is much greater than other forces like gravity and inertial forces so the particle follows the streamlines of the air. There is a point, if the streamline changes suddenly, that the inertial force of the particle is greater than the drag force. At this point, the particle will not follow the streamline. If this abrupt change in the air flow is near a surface the particle may impinge on that surface and thus deposition occurs. This behavior is obvious in air carrier sprayers. Chemical droplets are released into the air stream which transports them to the canopy where many are deposited.

To understand the relative importance of various parameters in air assisted chemical application a numerical model of particle behavior was developed. This model is described in detail in Appendix A. The model shows particle dynamics under various conditions in a theoretical flow. The model requires that an air flow field be defined. While it is easy to represent various theoretical flows, no good data exists about the actual flow fields from air assisted agricultural spray equipment. This model helped reinforce the belief that a clear understanding of the air flow must be obtained to assist further development of spraying equipment.

2.3 The Nature of Fluctuating Flows and Turbulence Generation

Almost all flow fields with any practical significance are turbulent at some scale. Turbulence is an ill defined word. Even many experts in the field admit the definition is elusive. What the layman may call turbulent may be defined simply as fluctuating flow to the true turbulence connoisseur. By the simplest definition turbulence is a fluctuating flow, making it very important to determine which fluctuation scales are of interest. It is easy to imagine a flow that is very smooth and constant on a large scale, but on a very small scale it is fluctuating. For most people this would still be a non-turbulent flow. While turbulence is subjectively defined, some general characteristics of turbulent flows are easily defined.

Turbulence is an irregular and fluctuating flow pattern. This flow pattern could be super-imposed on a very steady average flow and at one scale appear steady while at another appear turbulent. Turbulence can be thought of as many different scales of eddies superimposed on each other until virtually no discernible structure is apparent. There is a high degree of vorticity in a turbulent flow.

Turbulence is created by unstable velocity gradients. The most common generator of these gradients is a shear layer. Shear layers can be found at all points of the air delivery system. Examples of shear layers in an air carrier sprayer are: 1) at the fan blades, 2) between the diffuser walls and the air, 3) at the boundary between the jet plume and the still air, and, finally 4) as the air moves over the branches and the leaf surfaces. Each one of these shear layers creates its own turbulence and velocity fluctuations with different scales and intensities.

Turbulence is dissipative, it consumes energy. The kinetic energy of the fluid is converted to heat by the internal viscosity of the fluid. Turbulence decays if no energy is supplied. Usually, the energy for generating turbulence is obtained from larger scale fluid motion.

While turbulence is always decaying, shear layers are almost always present to create new turbulence; therefore, for practical purposes all fluid measurements must address the existence of turbulence to some extent. Turbulence can make measuring even the average flow very difficult. To determine the time scales for measurements we first need to know (paradoxically) the level and scale of turbulence. Large scale fluctuations of a flow are even more difficult to measure because the averaging must be able to preserve the large scales of interest but remove any unwanted effects of turbulent fluctuations.

2.4 Understanding Scales of Turbulence

To determine how to measure an air flow it is necessary to first have some understanding of what scale of the flow is important. A flow may appear perfectly smooth and steady at one scale and be quite turbulent at another scale;

for example, a table may appear smooth and flat, but when viewed with a microscope the surface appears rougher than a mountain range. A coffee cup would find the table smooth and flat, a dust mite would not. The air flow itself does not set the scale just like the table does not in the previous example; therefore, some external size scale of technological significance should be used to determine important scales of air flow.

In orchard chemical application important size scales are (in ascending order of size):

- Boundary layer over the surface of deposition
  - These scales are very small but will have a significant influence of the actual deposition of chemical on that surface.
- Leaf size
  - This scale would be important to bringing the chemical into the boundary layer.
- Air jet dimension
  - This scale is influences the mixing of the chemical across the air jet and turbulence generated at this scale has a great effect on the energy dissipated by the jet.
- Spray Machine size
  - This scale is important to even coverage of canopy and row to row penetration of the spray.
- Whole tree size
  - This scale influences the flow around whole trees, including vortices around the tree which may influence back side coverage.
- Whole orchard size
  - This scale is important to various characteristic flows within the orchard due to winds.

- Major weather pattern scales
  - This scale applies to even larger atmospheric flows such as prevailing winds.

Each one of these scales will have its own unique set of measurement tools which will produce the best results.

Vastly different scales of turbulence do not have a major effect on each other. Although the energy of one scale of turbulence is often generated by the motion of a larger scale, for measurement purposes it is reasonable to ignore or filter out flow scales that are far different from the one of interest. This is similar to other signal processing problems where filters are applied to a signal to remove unwanted "noise" or d-c offset. In air flow of sprayers, if the scale of interest is a jet size scale, then ignoring scales smaller than the leaf size and larger than the machine size would be a safe approximation. These other scales may still affect the measurements, but if these affects are understood, filters can be applied to remove any unwanted effects. The measurements should be capable of recording one major size larger and smaller than the scale of interest.

2.5 Determining Characteristic Frequencies of Turbulence

When instrumenting a turbulent flow the fluctuations will produce signals that can be analyzed by traditional signal processing techniques such as Fourier transforms. The study of the signal then becomes a frequency-based analysis. Viewing the signal in this fashion leads to the idea that the velocity fluctuations are occurring at certain frequencies based on the fluctuation's scale. As turbulent fluctuations are carried past a probe by the mean velocity, the fluctuation creates a signal of a certain frequency. A large turbulent motion or eddy would generate a low frequency fluctuation and a smaller eddy would generate a high frequency signal.

Understanding that certain scales of turbulence have certain frequencies of fluctuation leads to the question, "What is the frequency for a given size?" The answer is not completely clear, partly, because the mean velocity will also influence this frequency. The frequency will appear higher if the eddies are carried past the probe by a faster mean velocity. In addition, there is no one scale or frequency of turbulence. It is a broad spectrum with components all the way down to the smallest scale, where the viscosity of air destroys the motions. There is, however, a characteristic frequency where a peak in the energy of the spectrum can be found. Various empirical relations have been derived for certain common flows to help predict these characteristic frequencies.

Determining a sampling rate for the measurements requires that some estimate of the characteristic frequencies of interest be made. For jet flows Hinze (1959) gives a relation for the one dimensional energy spectrum based on Reynolds number of the jet velocity, size and kinematic viscosity. For all three machines used in this study at a distance of 0.5 m the jet velocities are below 26 m/sec (60 mph). Reynolds number for this jet based on 26 m/sec, 75 cm jet, and air as the fluid is $2x10^5$. Using this number the energy spectrum shows a characteristic frequency of approximately 50 Hz.

2.6 Moving Jet Flow vs. Stationary Jets

The forward motion of the sprayer as it is towed through the orchard generates a unique jet flow situation. Most common jet flows are roughly symmetric on both sides of the jet. The jet flows from a sprayer do not have symmetric conditions; the forward edge of the jet is being towed into still air while the trailing edge is exposed to air that has already been energized by the passing jet. This produces vastly different shear layers on the leading and trailing edge of the jet. To properly measure the air flow created by the air carrier agricultural spray equipment the jet must be moving so that the correct shear layers are produced.

The concept of the moving the jet and the rate of moving the jet is very important to air carrier sprayers. Various manufactures have tried to explain this to the operators of their equipment. The following excerpt from the FMC Operators Manual (1980) is a simple example of an explanation.

> If you place a lighted candle at one side of a room, and if you then stand at the other side and move an electric fan back and forth at a fast rate, the moving air will not reach the candle flame; and in the same way, if you move the air carrier sprayer too fast you won't fill the tree with spray-laden air.
>
> However, if you move the fan slowly, you give the moving air time to "bore a hole" in the room's atmosphere and reach the flame.

The forward movement of the sprayer influences the rate of displacement of air within the tree. It is important that operators understand this for calibration of the sprayer. It is also important that measurements be made on moving machines to reproduce actual operating conditions.

2.7 Techniques of Measuring Fluctuating Flow

The high-speed anemometers record almost instantaneous velocities. In a turbulent flow these velocities may have large fluctuations. A useful way to analyze this type of measurement is to consider each instantaneous velocity as a time-averaged velocity and a fluctuating component.

$$V_{inst} = V_{ave} + V_{fluc} \quad [2.7E1]$$

In standard turbulence notation for one-dimension this would be written:

$$\vec{U} = \overline{U} + u' \quad [2.7E2]$$

Potter and Foss, (1982) provide a good explanation of this concept. In a time varying flow the time over which to integrate to obtain V_{ave} must be carefully chosen. For this analysis, a period 10 times longer than the period of the turbulence of interest was selected.

Turbulence intensity indicates areas where the fluctuations are high compared to the mean. A turbulence number can be defined quantitatively by the root-mean-square value of the fluctuations (Kuethe and Chow 1986):

$$\text{Turbulence number} = \sigma = \frac{1}{\vec{V}_{mean}} \sqrt{\frac{1}{T} \int_0^t \frac{1}{3} (u'^2 + v'^2 + w'^2) dt} \quad [2.7E3]$$

Where: $\vec{V}_{mean}$ = the average fluid speed.

T = a time much greater than the fluctuations when compared to the mean.

u', v', w' = fluctuating components of the flow.

If the mean square values of the fluctuating components can be considered nearly equal then the turbulence number expressed as a percentage becomes:

$$\sigma \cong \frac{100}{\overline{U}}\sqrt{\overline{u'^2}} \qquad [2.7E4]$$

High turbulence number can help indicate areas of interest in a flow field such as large shear layers.

2.8 Three-Dimensionality of Turbulence and the Use of One-Dimensional Probes

Fluctuating flows and turbulence are inherently three-dimensional; however, many (in fact most) fluid dynamic measurements are made with one dimensional probes evidenced by the fact that good three-dimensional probes have only been developed very recently (Lukshiminarayuma, 1982). Again, an understanding of the goals of the measurements must be understood. Many flows are simply an average flow with fluctuations about the mean. As this average flow carries these fluctuations past the probe, information about the average velocity, amplitude and frequency of fluctuations can be recorded. The main requirement is that the probe is aimed in the direction of the average flow. A three-dimensional probe would actually yield little more information than a properly aligned one-dimensional probe. The turbulent fluctuations are random and will occur in any orientation. To obtain any useful information these fluctuations would have to be averaged and the only velocity left would be the average stream velocity. Breaking down the a signal into its average and fluctuating components. Algebraically for one dimension this is written as:

$$\vec{U} = \overline{U} + u' \qquad [2.8E1]$$

For three-dimensions:

$$\vec{U} + \vec{V} + \vec{W} = \overline{U} + \overline{V} + \overline{W} + u' + v' + w' \qquad [2.8E2]$$

If the probe is aimed in the direction of the average flow $\overline{U}$:

$$\overline{V} = \overline{W} = 0 \qquad [2.8E3]$$

so:

$$\vec{U} = \overline{U} + u' + v' + w' \qquad [2.8E4]$$

The only difference between 2.8E1 and 2.8E4 is that in the three-dimensional case there is information about v' and w'. The small scale structures of turbulence in most flows are, to the first approximation, independent of orientation or isotropic (Tennekes and Lumley, p. 65). The average fluctuations are equal:

$$\overline{u}' = \overline{v}' = \overline{w}' \qquad [2.8E5]$$

Unless instantaneous information about the actual structure of the fluctuation is desired the v' and w' are of little use as they are the same on the average as the u' information.

This analysis relies on the fact that the mean flow direction is basically known and that the probes can be oriented in that direction. In a wind tunnel this is very simple, the probe is aimed down the tunnel. For unconfined flow the average flow must be determined before the probes are aimed. Various techniques of flow visualization can be used to determine this average direction. A simple method is to hold a piece of yarn in the flow and the direction it points is parallel to the average flow.

2.9 Determining the Average Flow in a Varying Flow Field

The fluid velocity measurements taken by the computer are almost instantaneous velocity readings ($\vec{U}$). To analyze the data the signal needs to be broken down into average ($\overline{U}$) and the fluctuating components (u'). In a time varying flow field, care must be used to choose the proper way to produce $\overline{U}$, the average component.

Determining the average flow in a varying flow field requires an understanding of the scale that is important to the measurements. In a steady state flow determining the average flow is simply a matter of averaging over a long time period. In a varying flow field such as a passing jet a *local* average flow must be used. A time scale must be selected that will not remove too much detail of the bulk flow, but can average out the turbulent fluctuations. This average is needed to produce the $\overline{U}$ so the instantaneous velocity can be subtracted to produce the fluctuating term (u'). To do this an averaging *window* needs to be applied to the data. This will be a running average that produces the local $\overline{U}$. The averaging window chosen for these measurements was at least one order of magnitude greater than the fluctuation frequency of interest. Five data before and five data after an instantaneous velocity ($\vec{U}$) were used to produce $\overline{U}$.

2.10 Ensemble Averaging and Run-to-Run Variations

When a sprayer passes by an array of sensors, the probes take a *single snap shot* of the flow field. In a transient and fluctuating flow field it is unlikely that a single reading can characterize the flow field. Examining several passes is necessary to determine run-to-run variation of a particular field. Many times these readings are *assembled* into an ensemble average to obtain a larger sample. This is important for statistical calculations, but can lead to inaccurate conclusions when comparing flow fields. The ensemble average can smear out interesting characteristics of a particular field. Figure 2.10F1 illustrates a simple example of a problem created by ensemble averaging. Flow 1 is a narrow jet that changes angle from time, T1 to time T3. Flow 2 is a constant flow that emanates over the indicated area in all three times T1, T2 and T3.

In both Flow 1 and Flow 2 the ensemble averages look very similar, but the original flows are quite dissimilar. Again, the goal of the measurements must be understood before the measurement method is determined. If simple statistical information is all that is needed then the runs can be added and averaged at the time of acquisition. If other properties of the flow are interesting, such as instantaneous width of jet or variability of the flow then the individual runs have value and must be separately maintained.

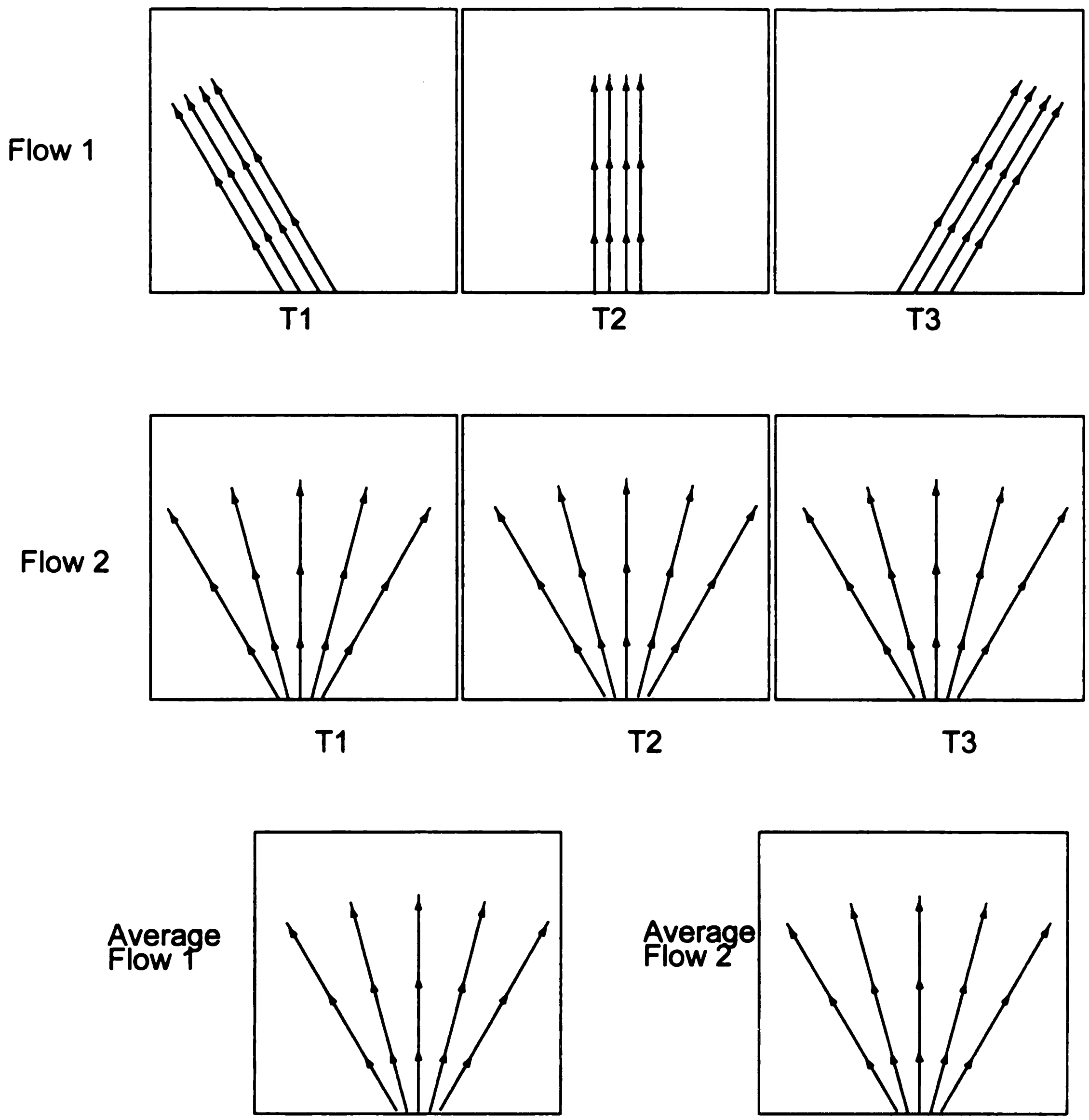

Figure 2.10F1: Information Loss Due to Ensemble Averaging

2.11 Transducers to Determine Flow Field Velocities

The transducer that this system uses to determine air velocity is a pressure sensing device. The pressure type of anemometer is very durable and does not require continuous re-calibration. With the implementation of piezoelectric pressure transducers and their high frequency response the pitot tube can be used and achieve a sampling frequency range high enough to begin to quantify turbulence. Since they are a true pressure device they can measure both the mean and fluctuating velocities.

2.11.1 Physical Considerations in Anemometer Selection

A pressure type transducer is less susceptible than other anemometers to physical damage from spray droplets, dust or other debris that may be in the air stream. Traditional methods of high frequency velocity measurements have usually been a hot-wire or hot-film. These devices use the cooling effect of the air passing over a surface to determine the velocity. Anything in the flow that can impact or adhere to the surface will at least change the measurement and often will destroy the instrument. These hot-wires and films must be re-calibrated on a daily basis even in a very clean laboratory environment.

Other anemometers, such as the cup or propeller anemometer, have a relatively low frequency response caused by of the mass of the rotor. Because of this problem, they are not suited for use in gathering turbulence data. They also pose a problem when placed in a tree canopy. The moving leaves may interfere with the rotor and yield inaccurate results.

Microphones are another type of pressure transducer that has been used to study turbulence. They have the frequency response to record the turbulence, but they lack the ability to read the mean flow component of the velocity field. They respond only to the dynamic part of the flow. This makes them unsuitable for determining the overall flow pattern of air-carrier spraying equipment.

Other factors that lead us to these transducers are cost and ease of use. The cost of the equipment is several times less than that of hot-wire or film systems. The transducers are internally amplified and temperature compensated; therefore, it is only necessary to hook up one four-wire cable between each transducer and the input of the data acquisition computer. This convenience changes the equipment from "delicate scientific equipment" to a usable tool that can be placed wherever the experimenter desires.

2.11.2 Using Pitot Tubes to Measure Air Velocities and Fluctuations

Pitot tubes have been used for air velocity measurement for many years. The air speed of an airplane is measured by such a device. Generally they are used for measuring average velocities in a single dimension. This is partly because the transient response of most pressure measurement equipment is relatively slow compared to a hot-wire anemometer. Before the advent of the hot-wire anemometer, much work was reported in which pitot tubes were used to measure complicated air flows. Blake (1976) summarizes and discusses various aspects of the use of pitot tubes for determining flow velocities and turbulence. Much of this work was abandoned with the development of the hot-wire due to its extremely quick time response and small size, despite the drawbacks mentioned earlier. The recent introduction of high speed pressure transducers has led us to reconsider the pitot tube for measuring complicated flows where durability and cost are important issues.

The pitot tube operates on the following principle. The fluid impacting on the open end of the tube is decelerated from its original velocity to zero since there is no flow in the closed tube (air is considered incompressible at this velocity). The energy of the moving fluid is *converted* to a pressure, due to the force that the fluid exerts on the end of the tube. This pressure is compared to the static pressure and the difference is the dynamic pressure. The Bernoulli equation,

$$P_1 + \rho \frac{V_1^2}{2} = P_2 + \rho \frac{V_2^2}{2} \qquad [2.11.2E1]$$

relates the pressure and velocity at two points along a single stream line. Where p_1 is the static pressure, p_2 is the dynamic plus static pressure and ρ is the density of air. V_1 is the velocity before reaching the tube and V_2 is zero, after reaching the end of the tube. By using the differential pressure P_{diff} and assuming V_2 is zero the equation can be written in this simple form:

$$V = \sqrt{\frac{2}{\rho} P_{diff}} \qquad [2.11.2E2]$$

This is the equation used to convert pressure measurements to velocities. The Bernoulli equation (2.11.2E1) assumes a steady state flow. Even though the flow we wish to measure is very unsteady it can be assumed to be *instantaneously* *steady.* This ignores that the flow may actually be accelerating or decelerating at the instant it was measured, but for these measurements the error is small and the calibrations against a hot-wire support this assumption.

Chapter 3

DESIGN AND CONSTRUCTION OF MEASUREMENT SYSTEM

3.1 Overview

To take field data the equipment ideally needs to be durable quick to setup and easy to use. The sensors should be capable of withstanding exposure to liquids, dust and rough handling. To resolve the desired scale of turbulence, the sensors and acquisition system must sample at a rate of 1000 Hz per channel and enough sampling locations must exist to provide a *fair* map of the flow field. The acquisition equipment and software need to be flexible enough to allow immediate analysis in the field and modification if necessary.

3.2 Pitot Tube – Pressure Transducer Probes

The system uses pitot tubes connected to pressure-to-voltage transducers for measuring air velocity. The reasons for choosing the type of anemometer are discussed in section 2.11. Design and construction systems are discussed below.

3.2.1 Physical Description of Probes

The pitot tube (a 12 cm metal tube) is connected to the pressure input port of the transducer and the other port is exposed to the static atmospheric pressure (Figure 3.2.1F1). This allows the transducer to measure the differential pressure between the dynamic pressure of the flow impacting the pitot tube and the static pressure of the atmosphere. The pressure sensing device, tubing and electrical connections are enclosed in a plastic case (a small toy football) for protection against the environment and handling. The probe is electrically connected to the data acquisition system via an RJ11 (modular telephone) plug and an LED on top of the probe allows immediate confirmation of the connection.

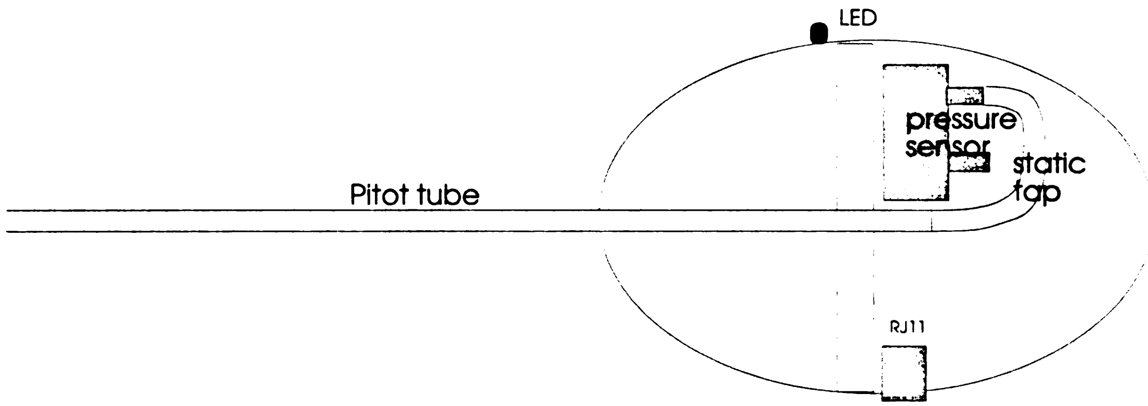

Figure 3.2.1F1: Physical Diagram of Pitot Tube Probe

3.2.2 Pressure Transducers

The pressure sensing units used are 160PC series Low Pressure Sensors manufactured by Micro Switch. They are capable of measuring 0-25 cm of H_2O (0-10 in. H_2O) with a linear correspondence of 1 vdc to 6 vdc output signal. The physical size is approximately 6 cm (2.4") by 3 cm (1.2"). The excitation voltage can range from 6 to 12 vdc. We are using 10 vdc supplied by the data acquisition computer.

3.2.3 Testing and Calibrating the Probes Against a Standard Hot-Wire

The pressure transducer equipment was tested against a hot-wire anemometer at Michigan State University's Turbulence Structure Laboratory.

The hot-wire anemometer is the current industry accepted standard for turbulence measurements. Comparing the pressure probes against a calibrated hot-wire anemometer shows that, for the frequencies of interest, pressure probes can follow the velocity fluctuations as well as to a hot-wire. The two pieces of equipment were positioned so that the hot-wire and the pressure tube were approximately 6 mm apart. The hot-wire sensor and the pressure sensor were calibrated against a Prandtl tube instrumented with a certified MKS Baratron type 398 differential pressure transducer. MKS is a brand of high quality pressure transducer, internally temperature-compensated, and precise to 4.5 digits. This transducer is very accurate, but does not have the dynamic response needed for turbulent measurements. Therefore, the calibration was conducted in a wind tunnel capable of producing 22 m/sec flow velocity with extremely low turbulence (0.3% free stream turbulence) (Falco, 1980). After the anemometers were calibrated over a range of zero to 22 m/sec the dynamic responses of the two instruments were compared in a turbulent flow. The equipment was exposed to a turbulent air jet and the response was recorded by the computer, sampling at 2000 Hz. The signal was digitally filtered to remove noise higher than 200 Hz. Figure 3.2.3F1 shows that the pressure transducer is able to capture the nature of the turbulent flow showing all the trends that the hot-wire anemometer shows. It is possible to discern the resonance that is characteristic of a pitot tube in a fluctuating flow. The average and standard deviation for both signals indicates that both transducer types are recording essentially the same flow despite this slight resonance.

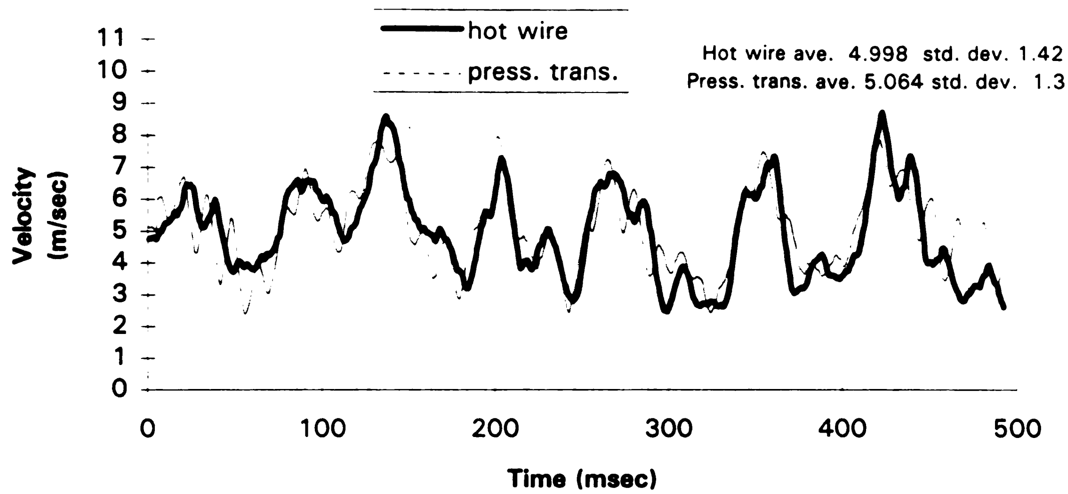

Figure 3.2.3F1: Hot Wire and Pressure Transducer in Turbulent Flow

The statistical method of showing this would be to perform a correlation calculation on the data. "A necessary and sufficient condition for the non-degenerate random variables X_1 and X_2, having finite variances, to be (properly) linearly dependent is that [the correlation coefficient is equal to] 1." (Wilks 1963). This is done by first subtracting the mean to leave only the fluctuations and determining a correlation coefficient for the two data sets. The correlation coefficient is defined as:

$$\frac{\text{covariance}\left(X_1, X_2\right)}{\text{variance}\left(X_1\right)\times\text{variance}\left(X_2\right)} \qquad [3.2.3E1]$$

Calculating the covariance on this data set of only 1000 points gives a correlation coefficient of 0.935.

3.2.4 The Effect of Varying Impingement Angle on the Probe

The probes are assumed to be aimed in the direction of the mean stream velocity, but there is no actual way to guarantee that they will be perfectly aimed. The angle that the air impinges on the end of the probe is of some concern. Literature suggests (Blake 1976) that pitot tubes are very good at angles from parallel of ±15 degrees. Tests were performed to confirm this with our probes. The tests were again run in Michigan State University's Turbulence Structure Laboratory low turbulence high speed tunnel. The probes were tested at 3 velocities and 4 angles. Figure 3.2.4F1 shows a plot of the percent of actual velocity vs. the angle of impingement off the free stream direction. These results confirm what the literature reports for pitot type probes.

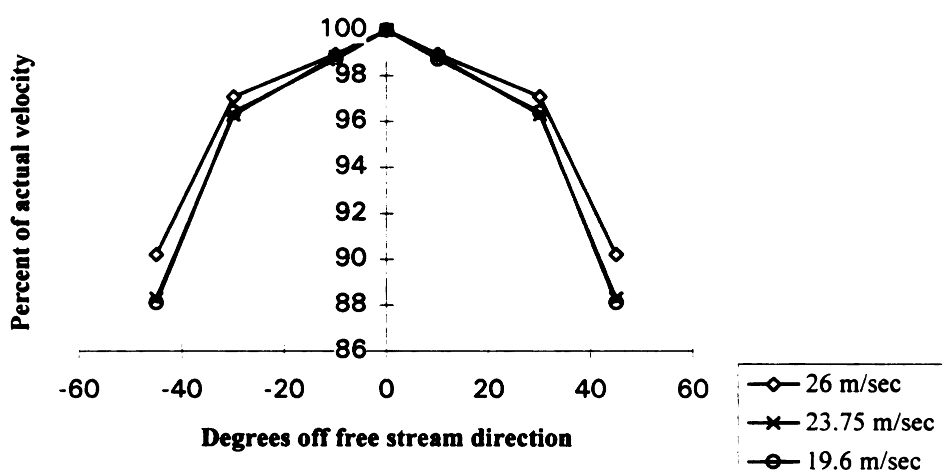

Figure 3.2.4F1: Probe Angle vs. Percent Velocity Loss

3.3 Data Acquisition Hardware

A PC computer-based acquisition system is used to record the signal produced by the transducers. Cost, portability, and availability of hardware and software components lead us to this choice. The computerization of the business world has lead to an incredible supply of low cost, but highly useful and easy to use software and hardware. Virtually any office computer has the computing capability and speed to take the data. Ironically, higher end office computers and graphic based software are selected for the same reason that the business world prefers them, ease of use. If data is easy to take, more can be taken in a given day and new areas can be explored that may not have been part of the original experiment.

The analog to digital converter is Advantech's PCL-818 Data Acquisition Card. This card is mounted on the PC bus in the computer. This is the actual data acquisition hardware, it is where the analog signals are converted to digital signals and vice-versa. It uses a 12-bit converter with a maximum hardware conversion rate of 100 thousand conversions per second. It features 16 channel analog input with software selectable gains, on-board timing, digital and analog output.

The card is wired to a panel that allows easy access to all 16 channels of input and output. The panel, manufactured by P.I. Engineering, Inc., has 16 RJ11 (modular telephone style) sockets. Each channel corresponds to a socket that has 4 wires: 1) An analog input line, 2) a digital output line, 3) a ground wire, and,

4) a 10 vdc source wire for transducers requiring a power source. This panel is designed to fit the standard 5¼ inch drive bay so the transducers simply plug right into the front of the computer.

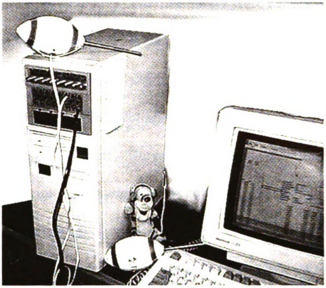

Figure 3.3F1: Data Acquisition Equipment

3.4 Data Acquisition Software

The data is imported directly from the data acquisition hardware to a spreadsheet through special software that links the acquisition card with the spreadsheet Excel. The software, developed by P.I. Engineering, Inc., Williamston, Michigan, is part of a complete system and includes facilities to easily control the system from Visual Basic. The data can be manipulated and displayed almost instantaneously in the field. This convenience makes it possible to perform analysis on the data and immediately discover problems. This is especially useful because mistakes can be corrected or new ideas explored while the experiment is still set up.

3.5 Calibration of the System

Calibration of all the transducers was performed in the high speed wind tunnel. Individual calibrations of each transducer help eliminate any differences in manufacture of each unit. These transducers were calibrated against a certified precision anemometer at the Turbulence Structure Laboratory.

MicroSwitch the manufacturer of the pressure transducers claims a linear relation between pressure and voltage; however, when the actual relation is plotted it is not exactly linear. The entire system, including the assembled probes, wires and data acquisition system, was calibrated against the laboratory's 4.5 digit MKS pressure transducer anemometer system in the high speed low turbulence wind tunnel. These were calibrated using 12 velocities over the complete range of the tunnel's capability (0-26 m/sec mph) (Falco 1980). At each velocity the system was allowed to reach steady state and time averages of 3000 points for one minute were used to achieve a very stable velocity reading. The calibration equations are shown in Table 3.5T1 and are used in Microsoft Excel for the voltage-to-pressure conversions necessary to determine velocity. Two transducer models were used, they have different calibration equations but are similar in basic specifications.

Table 3.5T1: Calibration Equations for Pitot Transducers

MB Type	
M1	8.320711*((VOLTS+6)^2-(ZERO+6)^2)^(0.5)
M2	9.352166*((VOLTS+6)^2-(ZERO+6)^2)^(0.5)
M3	8.307291*((VOLTS+6)^2-(ZERO+6)^2)^(0.5)
M4	8.228605*((VOLTS+6)^2-(ZERO+6)^2)^(0.5)
M5	3.634566*((VOLTS+6)^2-(ZERO+6)^2)^(0.5*(1+VOLTS/9))
M6	9.396534*((VOLTS+6)^2-(ZERO+6)^2)^(0.5)
M7	7.821944*((VOLTS+6)^2-(ZERO+6)^2)^(0.5)
M8	8.452369*((VOLTS+6)^2-(ZERO+6)^2)^(0.5)
PT Type	
P1	44.04544*(VOLTS-ZERO)^0.5
P2	45.75142*(VOLTS-ZERO)^0.5
P3	43.23935*(VOLTS-ZERO)^0.5
P4	49.64643*(VOLTS-ZERO)^0.5
P5	45.41569*(VOLTS-ZERO)^0.5
P6	44.95737*(VOLTS-ZERO)^0.5
P7	46.17535*(VOLTS-ZERO)^0.5
P8	49.10776*(VOLTS-ZERO)^0.5
P9	43.12217*(VOLTS-ZERO)^0.5

Chapter 4

FIELD PROCEDURES

4.1 Overview

The measurement system described in chapter 4 was used to measure three sprayer models at Michigan State University's North West Horticulture Research Station (NWHRS), near Traverse City, Michigan. The availability of equipment and access to several protected field sites made NWHRS an ideal location. Preliminary data was taken in August of 1993 which led to the optimization of techniques for collecting the presented data which was acquired in August of 1994. This chapter describes the procedures used to set up, acquire and store the data, as well as describing the operating conditions and type of equipment tested.

4.2 Equipment, Placement and Operating Environment

4.2.1 Probe Poles

Fifteen probes of the type described in Sec. 4.1 were attached to a pole 5 meters in height. The probes were attached at 25 cm distance starting at 1 meter from the bottom of the pole. The probes were connected to the data acquisition computer using equal length wires (the same wires used in the calibration) to ensure the same excitation voltages for each sensor. The pole was attached to a pallet at the base and held upright by 3 guy ropes. See Figure 4.2.2F1 for a pictorial diagram of the setup.

4.2.2 Probe Aiming

As stated earlier the aiming of one dimensional probes is important to probes measurement of the flow. The probes must be aimed in the direction of the average bulk flow. Earlier experiments with a yarn tuft array indicated that the average bulk flow for both types of sprayers emanate from the fan axis. The yarn tufts were attached to chicken wire held in a frame; 4 cm yarn pieces attached at regular intervals. The direction that the yarn pointed indicated the direction of the average bulk flow. For the radial types this was a radial pattern and for the crossflow type this was perpendicular to the fan axis. Figure 4.2.2F1 shows the aiming of the probes for the two types of sprayers. This probe aiming is similar to the aiming method used by Salyani and Hoffmann (1996).

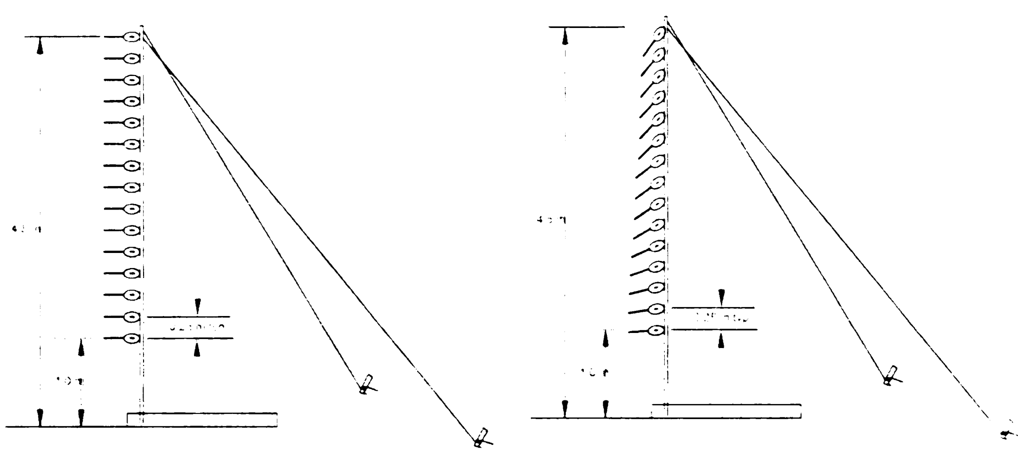

Aiming for Tower-Crossflow Type Sprayer

Aiming for Radial Type Sprayer

Figure 4.2.2F1: Probe Aiming Diagram

4.2.3 Tractor Trigger Probe

To ensure that the commencement of the data was the same for each run, a trigger probe was used to trigger the computer when the tractor was in a certain position. This trigger was a piece of flexible tubing attached to a pressure transducer. The signal from the transducer was connected to the 16th input channel on the computer. A pressure spike on this channel indicated that the tractor wheel had contacted the sensor and the data acquisition was started. This signal was also used to measure the speed of the tractor by timing the time between the front wheel and the rear wheel pressure spikes.

4.2.4 Computer and Power System

The data acquisition computer was a 486-33 MHz computer with DOS operating system and running Windows graphic user interface. The analog to digital system was a 12 bit system and is described in detail in Sections 3.3 and 3.4. This was the same computer as used in the laboratory calibration. In the field it was powered by a small portable 110 volt 60 Hz AC generator, Yamaha model EF1000 rated at 850 VA.

4.2.5 Tractor Type and Operating Conditions

The towing tractor used for all three sprayers was a 1994 Ford model 4430. It has a rated output of 52 kW (70 Hp). It was operated in 4 wheel drive on basically level ground to minimize wheel slip.

4.2.6 Ambient Local Weather Conditions

The measurements presented were taken in a two day period. A site was selected that had wind breaks and hills that help reduce wind. During these experiments the ambient wind conditions were not noted over 0.9 m/sec (2 mph). The temperature range for both days was between 20° C to 24° C (68° F and 76° F).

4.3 Spray Equipment Tested

Three sprayers were tested. Two conventional radial type and one experimental tower type air carrier orchard sprayers were used for the tests.

4.3.1 Curtec, 3 Point Hitch Model

The unit that was tested was an experimental 3 point hitch model crossflow fan model. This unit was designed and built by Michigan State University's Agricultural Engineering Department in 1994. It uses the same technology and fan design as the larger commercially available Curtec sprayers built by BEI, Inc., South Haven, Michigan.

- Specifications:
  - Mounting Type: 3 point hitch mount.
  - Power supply: PTO hydraulic pump.
  - Nominal power required: 18.6 kW (25 Hp).
  - Fan Type: Vertically mounted, hydraulic powered crossflow.
  - Atomizer Type: Hydraulic powered, 5500 rpm direct drive rotating basket type.
  - Maximum air exit velocity: 26 m/sec (60 mph).

- Diffuser, shroud type: Formed fiberglass.

- Other notable features: The unit has three 122 cm (48 inch) fans which can be adjusted to different angles. The fans were set at zero angle (fan axis perpendicular to the ground) for this experiment. This unit sprays only to one side (right side).

4.3.2 AgTec

The unit tested was an AgTec model 400 PC. Manufactured about 1988 by AgTec Div., Ag-Chem Equipment Co., Inc., Minnetonka, Minnesota.

- Specifications:

  - Mounting Type: 2 wheel trailer.

  - Power supply: standard PTO shaft.

  - Nominal power required: 37 kW (50 Hp).

  - Fan Type: belt driven centrifugal horizontally mounted with axis perpendicular to direction of travel.

  - Atomizer Type: 16 air shear nozzles.

  - Maximum air exit velocity: 89 m/sec (200 mph).

  - Diffuser, shroud type: Formed fiberglass with sheet metal deflector.

  - Other Notable features: Fan pressurizes a plenum which is ducted out through the formed diffuser at the rear of the machine. The high exit velocity is critical to the atomization of chemical.

4.3.3 FMC

The unit tested was an FMC model LV320. Manufactured circa 1980 by FMC Corporation, Ripon, California.

- Specifications:

  - Mounting type: 2 wheel trailer.

  - Power supply: standard PTO shaft through gear box to fan.

- Nominal power required: 30 kW (40 Hp).
- Fan type: 74 cm (29") diameter 12 blade axial flow, mounted with axis horizontal and parallel to the direction of travel, operating at 2300 RPM.
- Atomizer type: 14 standard fluid pressure disc/core hollow cone nozzles.
- Maximum air exit velocity: 49 m/sec (110 mph).
- Diffuser, shroud type: Stamped aluminum with sheet metal struts and deflectors.
- Other notable features: Unit is known to produce drastically different air properties on each side.

4.4 Field Data Collection and Analysis

This section describes the procedures that were used in the field to obtain the data.

4.4.1 Repetitions

Each "run" or data set required approximately 3 to 5 minutes to complete. This involved mainly repositioning the tractor and resetting the computer for the next run. A minimum of 4 repetitions of each variation was recorded. Since the data acquisition computer can immediately display the results of a run, runs that had problems (such as a trigger failure) were rejected. This ensured at least 4 viable runs for each condition under test.

4.4.2 Distance from the Probe Pole

To map the jet plume, the probe pole was successively placed 1.5 m, 2.5 m, 3.5 m and 4.5 m from the machine center and data were collected for each machine and condition. Lines were drawn on the ground at these distances to help the tractor operator aim the tractor properly. Figure 4.4.2.F1 shows these positions.

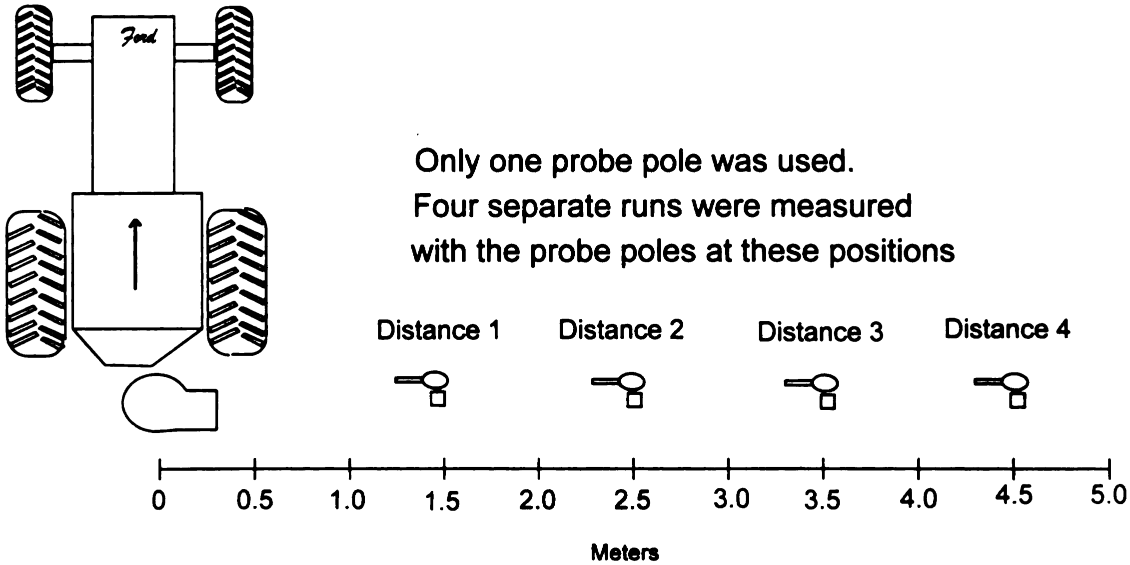

Figure 4.4.2F1: Probe Pole Placement Relative to the Equipment

4.4.3 Varying Tractor Towing Speeds

To observe the effect of different tractor speeds two different speeds were recorded. One speed was approximately 6.1 kph (3.8 mph) and the other was 7.3 kph (4.5 mph).

4.4.4 Corrections for Far Plume Drift

The jet plumes from some machines are not perpendicular to the direction of travel. At 4.5 meters from the sprayer, the plume missed the probe pole if the trigger position was the same as that used for the closer runs. In these cases the trigger was moved and the position was noted so during analysis the new position could be compensated. In one case the plume was aimed forward and the other machine the plume was aimed back.

4.4.5 Data Acquisition and Sampling Frequency

Two programs were directly involved in the data acquisition. A small Visual Basic program (written specifically for this project) and Microsoft Excel where the bulk of the data storage and signal processing takes place.

The Visual Basic program had four functions:

1. Turn on an indicator light to signal the tractor operator to begin the next run.
2. Monitor the trigger sensor to determine the time between the front wheel pulse and the rear wheel pulse to determine actual tractor speed.
3. Activate Excel and record the tractor speed, run number and file name to the spread sheet.
4. Begin the collection of data on the velocity probe channels.

On the second trigger Excel began recording data for 3 seconds at 1000 Hz on all 15 velocity probe channels. A sampling frequency of 1000 Hz was chosen because one of the objectives was to examine the delivery of the air from the sprayer to the canopy. The most important scale for this is the air jet scale. The characteristic frequency of this scale for these jets is approximately 100 Hz. Refer to section 2.5 for a detailed explanation of characteristic frequencies of turbulence. The 1000 Hz data provided sufficient over sampling to allow digital filtering and averaging necessary to remove any noise at frequencies above 100 Hz.

4.4.6 Initial Conversion of Voltage Signals to Velocity Data

After sampling at 1000 Hz, the data was immediately filtered to reduce the data set size and remove any unwanted high frequency noise. Every 10 points of sample were averaged to produce one value. This reduced the 45000 point data set by a factor of 10. The data for each channel was converted to velocity data using the calibration equations determined and explained in Section 3.5. Velocities were plotted on a graph in Excel during the acquisition so that any problems could be found while the experiment was still underway. Viewing the data immediately revealed errors such as missed triggers, malfunctioning sensors or an inappropriate analog range. Problems could be immediately corrected, ensuring that all saved data sets were valuable. Appendix C shows a sample data sheet as it appeared on the screen during the recording of the data.

4.4.7 Data Storage

The data was first stored in individual Excel files on two resident hard drives in the data acquisition computer. At the completion of a set of runs the data was also transferred to a 90 Megabyte Bernoulli backup drive. The working data and files were maintained on the internal hard disks.

Chapter 5

ANALYSIS AND PRESENTATION OF DATA

5.1 Introduction

The analysis and presentation of complicated three-dimensional flow fields is extremely difficult. Many people in various disciplines have tried to produce an acceptable method and this is one more attempt. For stationary fans ASRA has developed a simple method of producing iso-velocity lines (lines of constant velocity) in a certain plane. In a three-dimensional jet moving transversally this becomes much more difficult. To achieve a visualization of the jet flow, the data was assembled into arrays of the discrete measured points. Three-dimensional linear interpolation was used to create cross-sections of the jet for visualization.

The basic steps used for data reduction and analysis are outlined below. A detailed explanation for each step is presented in the following sections.

1. Record the raw voltages from pressure transducers.
2. Digitally filter and reduce data set from 1000 Hz to 100 Hz.
3. Convert the data to pressures using calibration equations.
4. Convert pressures to air velocities using Bernoulli principles.
5. Separate velocities into mean and fluctuating flow components.

6. Select and combine mean velocity arrays from 4 measurement distances to make one data set.

7. Convert time values into distances.

8. Create a discrete 3-D spatial array of velocity points.

9. Choose and define 2-D cross-sections of jet for display.

10. Use linear interpolation to create a continuous field from the discrete data.

11. Create an array from the defined plane and the interpolation routine.

12. Plot the array using a surface plot with color representing the velocity values.

13. Display plots in diagrams to size scale with equipment tested.

5.2 Recording and Converting Voltages to Air Velocities

The data was collected as using the equipment described in chapters 3 and 4. The sampling frequency of 1000 Hz was used to obtain the initial data. The data was acquired over a 3 second interval on 15 independent channels. This generated a data set of 45,000 for each run at one measurement distance. This data was immediately reduced by 10 times by averaging every 10 points to obtain one average point at a 100 Hz rate. This is a block averaging method and is represented mathematically by Equation 5.2E1.

$$V_i^A = \frac{1}{N}\sum_{n=0}^{N-1} V_{Ni+n}^M \qquad [5.2E1]$$

Where: $i = 0 \ldots n-1$.

V^A = block average voltage.

V^M = measured voltage.

Averaging served two purposes, first it reduced the data to a more manageable size. Second it "filtered" the data to 100 Hz which is the highest frequency of interest in this flow. This frequency was determined by studying the one dimensional characteristic turbulent frequencies of jet flow, see section 2.5 for details. Although the pressure transducers have a higher frequency response, the complete calibrated probes were shown to have a very good correlation to traditional hot wires at frequencies lower than 100 Hz, this is shown in section 3.2.3.

The raw voltages are converted to air velocity. This is done by using the equations described in section 3.5. These equations are based on the Bernoulli principle for converting dynamic pressure to velocity (section 2.11.2). Each transducer was individually calibrated against a known air velocity in an extremely low turbulence wind tunnel. Individual calibration constants were used for each transducer when converting the voltages to velocities (see Table 3.5T1).

Pitot tubes only measure velocities in a positive direction, they can not measure negative velocities. In the fluctuating flow of the sprayer jet the probes occasionally register negative pressures. These pressures may be real, probably caused by turbulent swirls producing slight suction on the tube. The negative values can not be converted to legitimate velocities. The negative pressures occur when the mean velocity is on the same order of magnitude as the fluctuating velocity. This occurs when the flow is essentially zero, such as at the leading or trailing edge of the jet. If the pressure value was negative it was assumed to be zero for analysis purposes. This was done for two reasons, first, the pitot tube does not produce valid negative values and second the basic equation to convert pressure to velocity takes the square root of the pressure. Mathematically, negative pressures would produce imaginary velocity values. Therefore the equations to convert the voltages to velocities are of the form:

$$U_i = \begin{cases} C_{wt} \times \left(V_i^A - V_0\right)^{\frac{1}{2}} & \text{if } V_i^A > V_0 \\ 0 \quad \text{if } V_i^A < V_0 \end{cases} \qquad [5.2E2]$$

Where: C_{wt} = wind tunnel calibration constant.

V^A = block average voltage.

V_0 = zero velocity voltage.

U = air velocity.

The instantaneous measurements were separated into an average (mean) flow and a fluctuating component. The theory for this is discussed in section 2.7. Determining the "average" velocity in a transient flow is difficult. If the averaging period is too long the nature of the transient flow is lost. A period of one order of magnitude larger than the characteristic turbulent scale was chosen. A running average on 11 points was used to create the mean flow component. The running average uses 5 points previous and 5 points after the time of the average point produced. This does not reduce the data set size but "smoothes" it.

$$\overline{U}_i = \frac{1}{11}\sum_{n=-5}^{n=5} \vec{U}_{i+n} \qquad [5.2E3]$$

Where: $\overline{U}_i$ = local mean velocity.

$\vec{U}_i$ = instantaneous velocity.

The fluctuating component was calculated by subtracting the instantaneous velocity from the mean velocity.

$$\vec{U} - \overline{U} = u' \qquad [5.2E4]$$

The mean velocity component was used to plot the velocity maps shown in Section 5.6.

Recording and converting the voltages to velocities was done in Microsoft Excel when the initial data was obtained. Figure 5.2F1 shows the mean velocity ($\overline{U}$) for one sensor measuring a Curtec sprayer at 2.25 m height. Fifteen such mean velocity series were recorded for each run, one for each sensor.

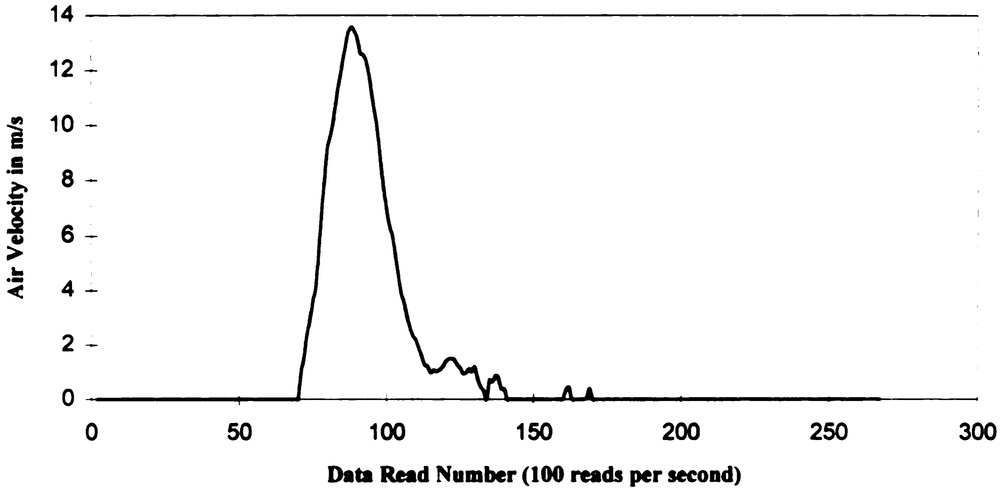

Figure 5.2F1: Mean Velocity Profile of One Sensor

5.3 Assembling the Data Sets for Display

The air jet was measured at four different distances from the sprayer outlet (Section 4.4.2). These four distances were not measured simultaneously. a separate 'run' was made for each distance. To obtain a complete map of the flow, one run from each distance was arbitrarily selected. These 4 data sets were used to make one 3-dimensional array. The 4 data sets were used as input to a program that generates 2 dimensional slices of the 3-D data field.

The final data set represents a 3-D region approximately 2 m × 3 m × 3 m. The actual number of data points for each of the three-dimensions are very different. In the X direction there are 300 points (due to recording frequency) in the Y direction there are 15 points (number of sensors) and in the Z there are only 4 points (number of different distances measured). This is illustrated in Figure 5.3F1.

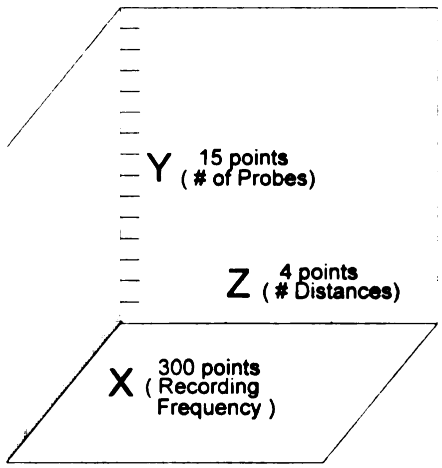

Figure 5.3F1 Resolution of Each Axis in Measurement Region

5.4 Converting Recording Frequency to Distance

Traditionally, to measure a jet an array of sensors was assembled and moved past a stationary fan generated flow. It is assumed that the jet is more less constant and the array will measure different parts of the flow at different times but the assembled measurements will represent average jet flow. In our case we moved the sprayer past a stationary array of probes. This was done to generate the desired actual flow field and allowed our sensors to "sweep" the flow. To regenerate a representation of the flow field the forward motion of the sprayer needs to be translated into a traverse coordinate of the measurement. In a sense the time coordinate is transformed into a space coordinate through the use of the sprayer speed. This type of transformation is used commonly in fluid mechanics in the study of turbulent structures. When studying turbulence it is assumed that the structure of interest is being carried past a probe by the mean flow. The *Taylor's hypothesis* or "*Frozen Flow Hypothesis*" is used to transform time into space coordinates. The substitution of time for distance over average velocity is good when the fluctuations are small compared to the average velocity (Hinze, 1959, sec 1.8, Tennekes and Lumley, 1972, p. 253). A similar transformation allows us to transform the time of a probe's read to a position relative to the jet using the sprayers forward motion speed. The probes are triggered to begin recording at a certain time by a physical position on the tractor. Thus if the sprayer is moving forward at a constant rate this is like the probe moving back at the same rate. If the rate is known then the distance traveled between data samples determine the effective distant between the probes traverse reads. The equation for this transformation is simply:

$$\Delta x \cong \frac{\Delta t}{S_T} \qquad [5.4E1]$$

Where: Δx = distance traveled between data samples.

Δt = time between samples.

S_T = towing speed.

At the filtered sampling rate of 100 Hz and a towing speed of 1.69 m/sec equation 5.4E1 yields a resolution of 0.6 cm in the X direction.

5.5 Iso-Velocities

The data taken is a representation of scalar velocities taken at several spatial points in the flow field. The representation is difficult for the human to interpret. We desired to represent this field with lines and surfaces of constant velocities. Much the same as standard data for commercial fans is presented (Grainger, 1996).

For visualization purposes these discrete velocity points were used to create continuous iso-velocity lines on planes which cut through the 3-dimensional velocity field. This was done by selecting a plane of interest. For a X-Z plane the height of 1.8 m above ground was chosen. For the Y-Z plane a plane that passed through the highest velocity of the X-Z plane was used. Figure 5.5F1 shows these planes in relation to the equipment tested.

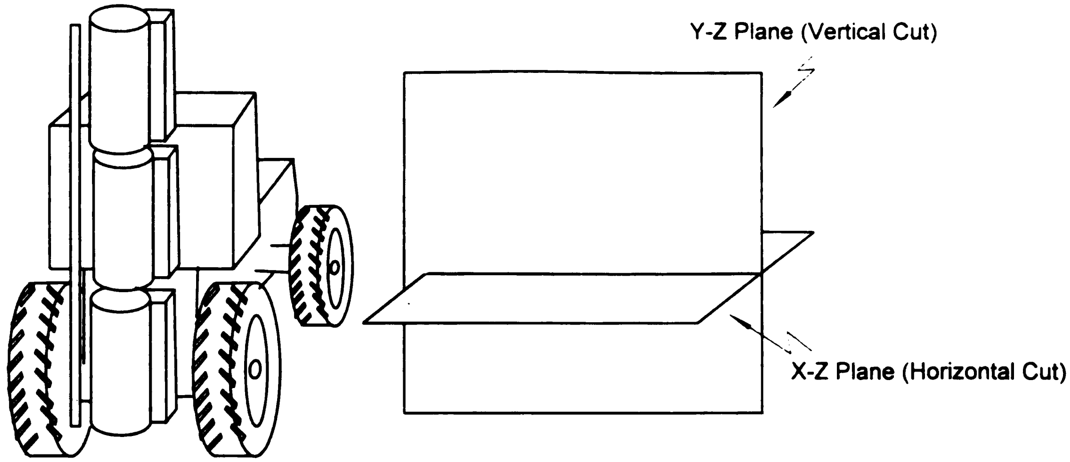

Figure 5.5F1: Visualization Planes in Relation to the Equipment Tested

A small program was written to combine 4 data sets, convert the time dimension to a space dimension and use linear interpolation to produce an uniform array of velocity points in the defined plane. The program output is a simple ASCII file for plotting. The code for this program is shown in Appendix B. The results were imported to Excel and plotted using a three-dimensional graph with the horizontal and vertical axis representing distance and the color representing the air velocity. These results are displayed approximately to scale with a diagram of the equipment tested in the following section.

5.6 Three-Dimensional Presentations

The results of this analysis are presented for the three air carrier sprayers tested. A single mean iso-velocity plot is shown with each sprayer to visualize the scale and 4 runs are displayed in the next figure to show run to run variation. Both horizontal and vertical cuts are shown and the machines are presented in alphabetic order.

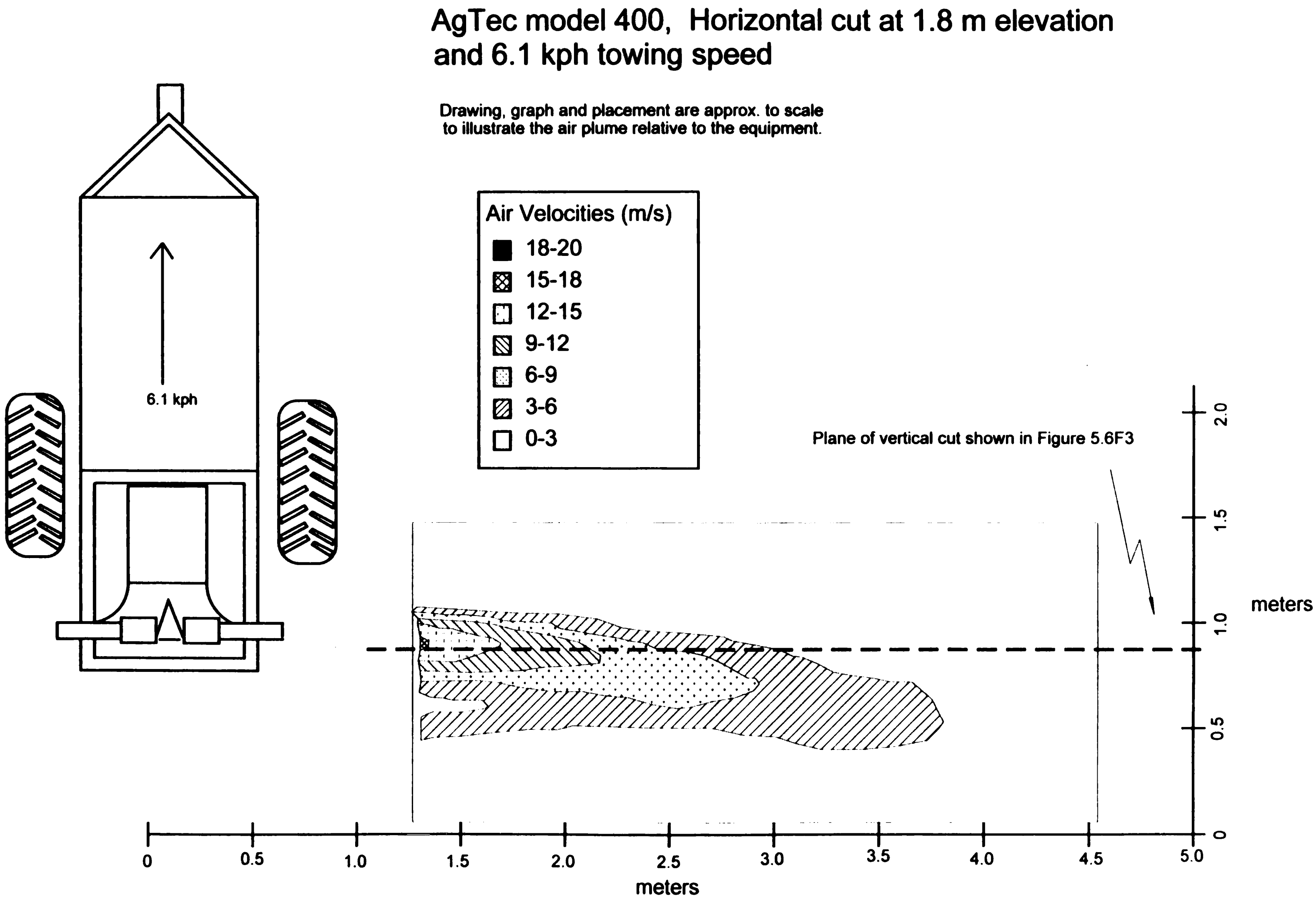

Figure 5.6F1: Iso-Velocity Plot, Horizontal Cut, AgTec Model 400

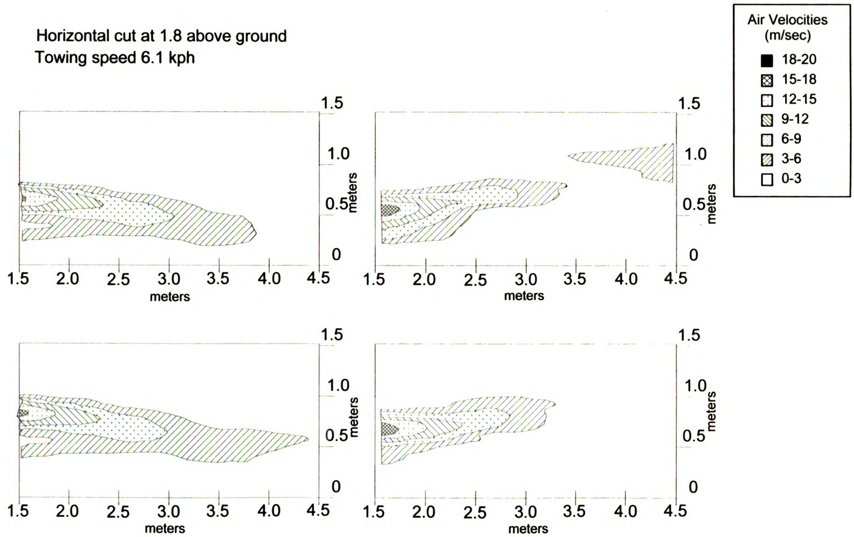

Figure 5.6F2: Variation of Iso-Velocity Plot, Horizontal Cuts, AgTec Model 400

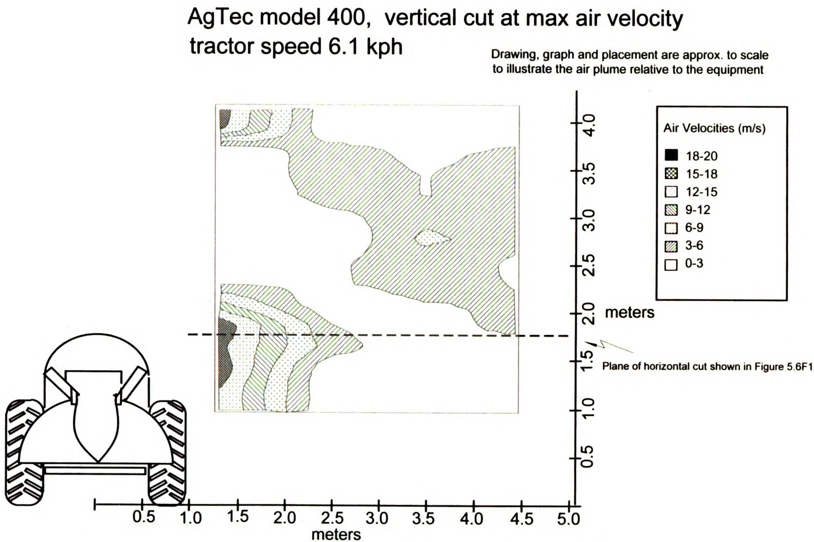

5.6F3: Iso-Velocity Plot, Vertical Cut, AgTec Model 400

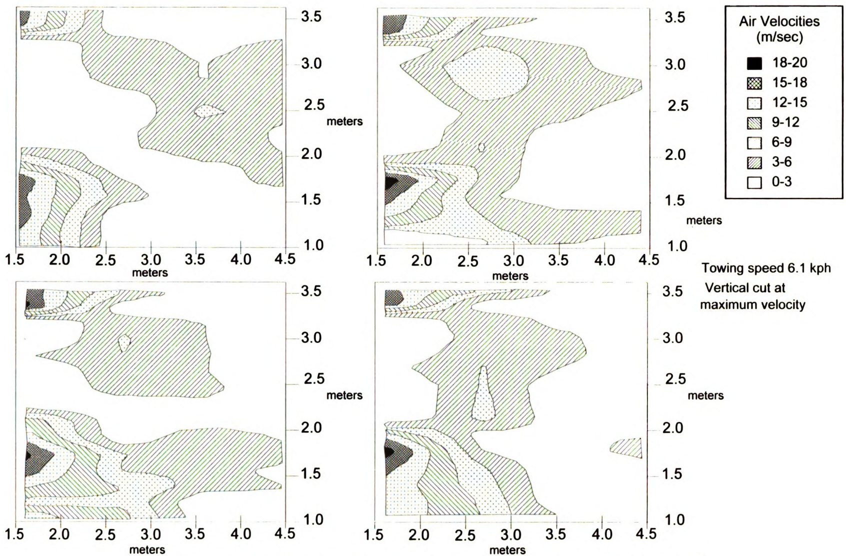

Figure 5.6F4: Variation of Iso-Velocity Plots, Vertical Cuts, AgTec Model 400

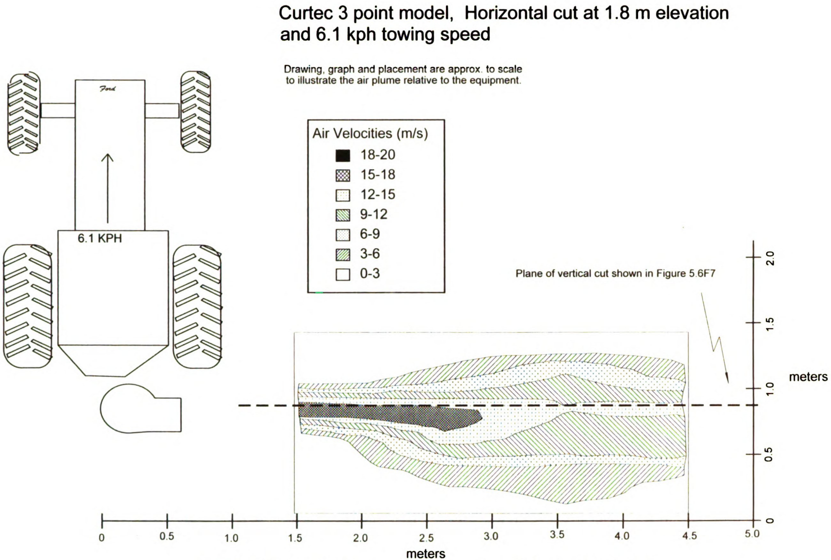

Figure 5.6F5: Iso-Velocity Plot, Horizontal Cut, Curtec 3 Point Model

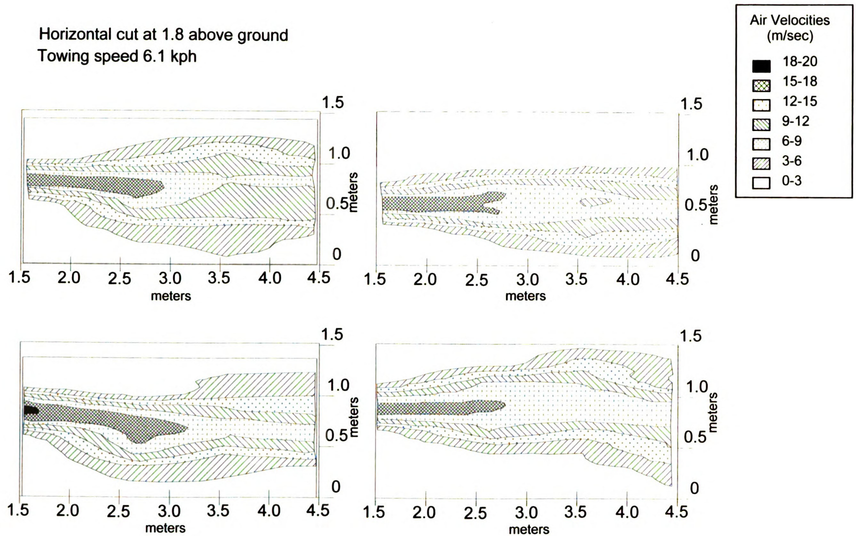

Figure 5.7F6: Variation of Iso-Velocity Plots, Horizontal Cuts, Curtec 3 Point Model

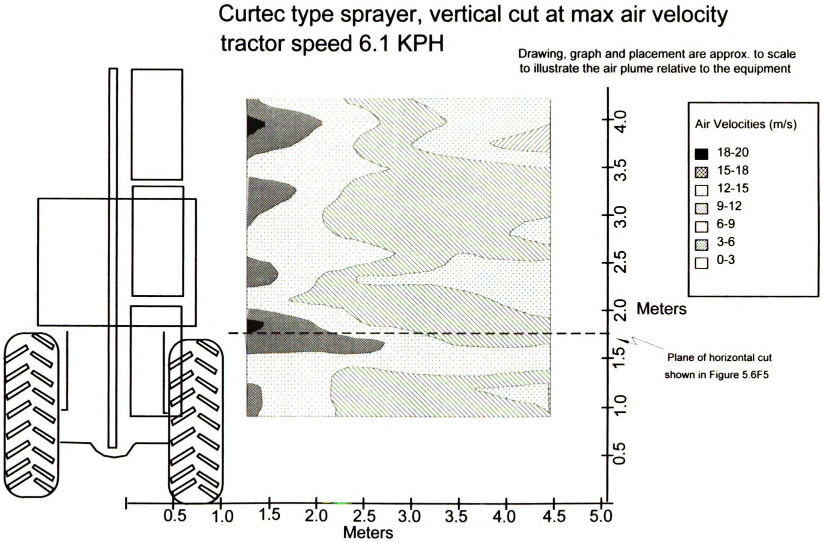

Figure 5.6F7 Iso-Velocity Plot, Vertical Cut, Curtec 3 Point Model

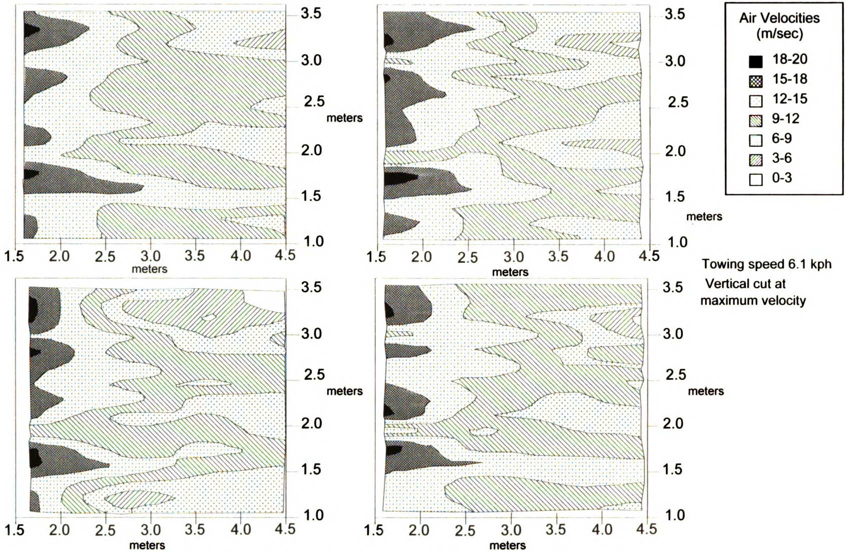

Figure 5.6F8: Variation of Iso-Velocity Plots, Vertical Cuts, Curtec 3 point Model

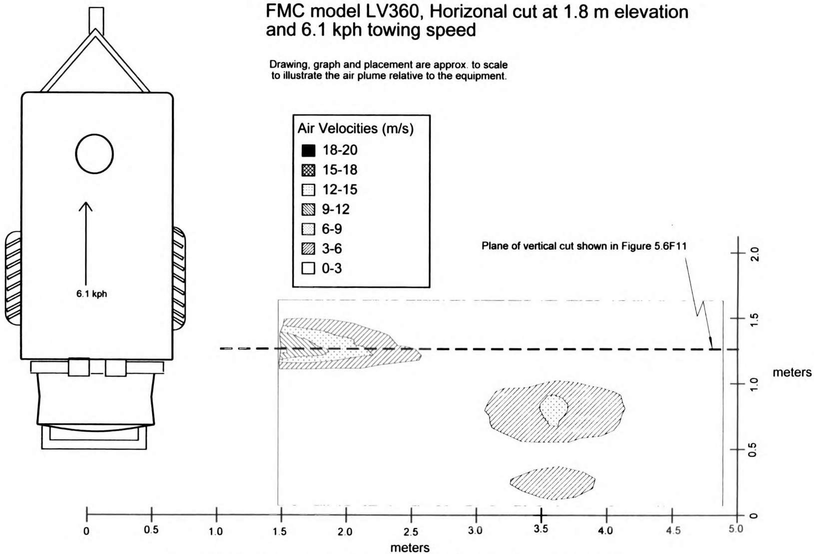

Figure 5.6F9: Iso-Velocity Plot, Horizontal Cut, FMC Model LV360

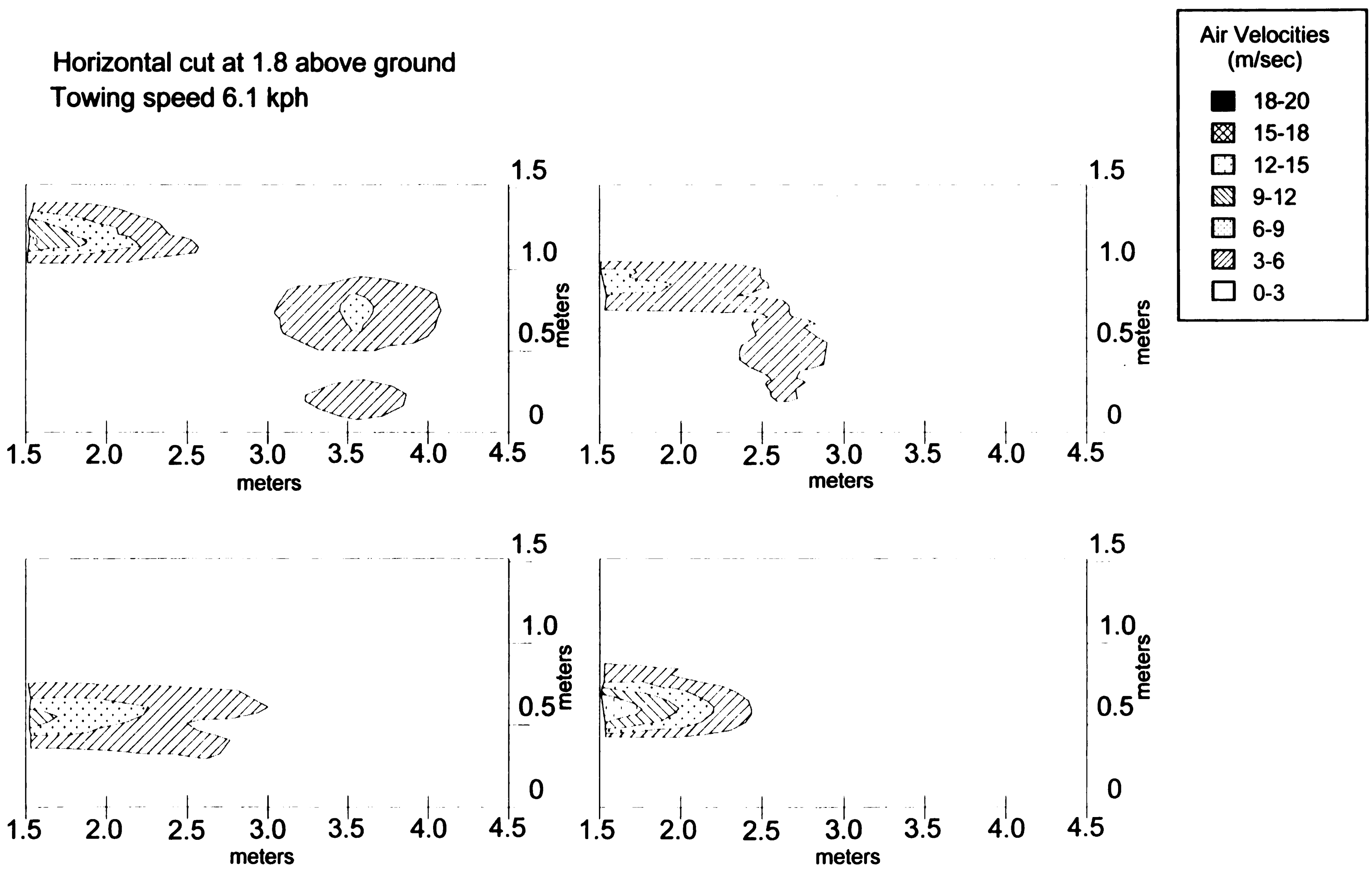

Figure 5.6F10: Variation of Iso-Velocity Plots, Horizontal Cuts, FMC Model LV360

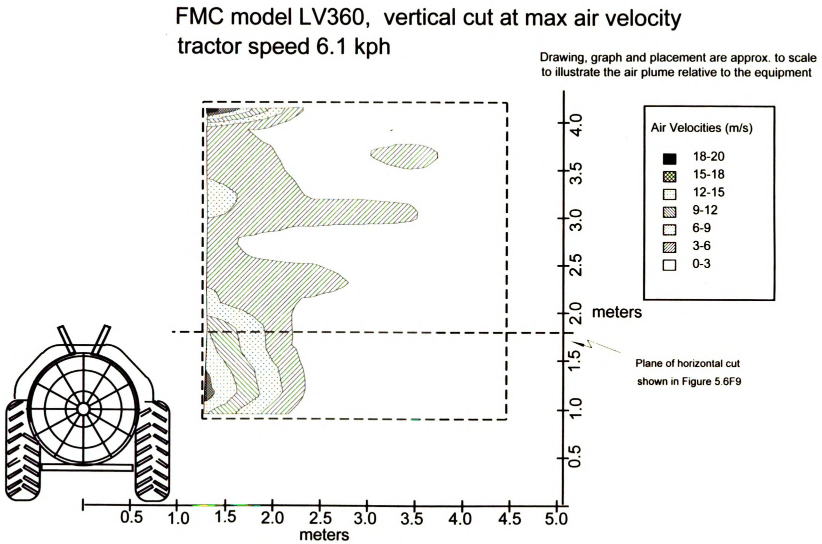

5.6F11 Iso-Velocity Plot, Vertical Cut, FMC Model LV360

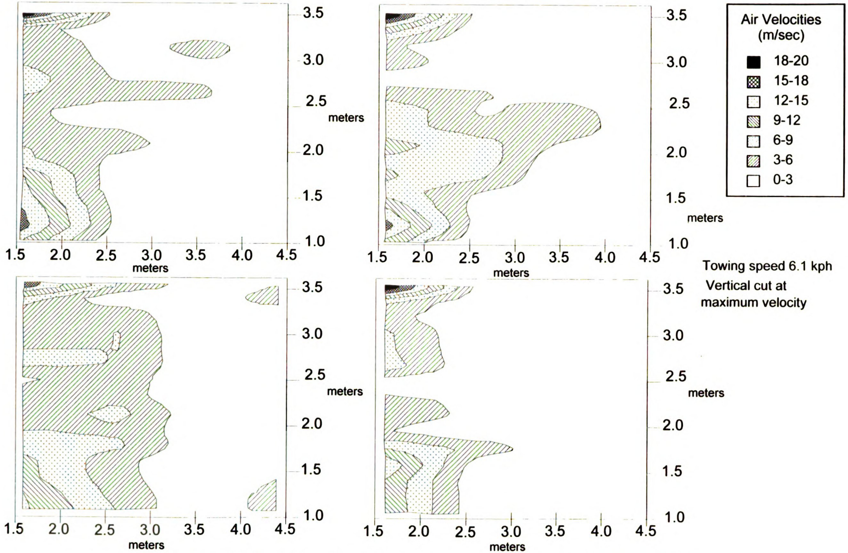

Figure 5.6F12: Variation of Iso-Velocity Plots, Vertical Cuts, FMC Model LV360

5.7 Comparing Two Towing Speeds

This measuring technique can be used to study the sensitivity of the pattern to various parameters such as towing speed. Figure 5.7F1 shows the Curtec and AgTec sprayer patterns at two different towing speeds.

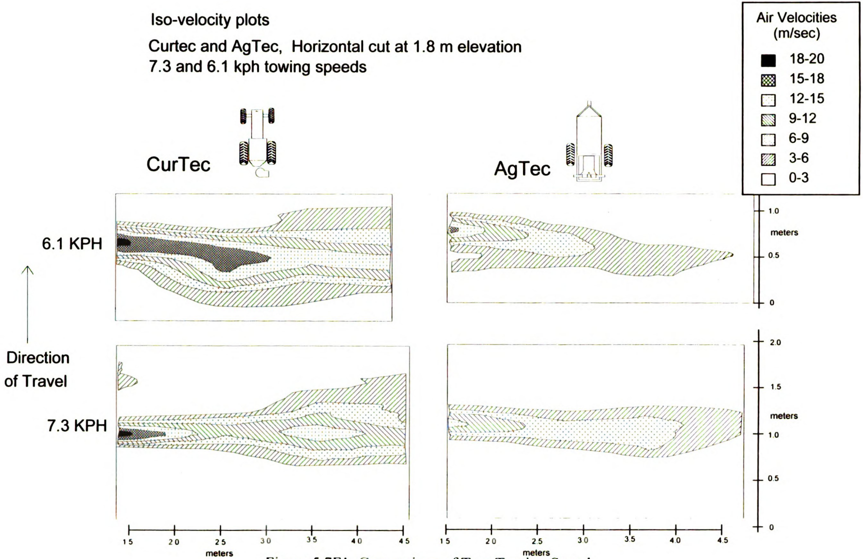

Figure 5.7F1: Comparison of Two Towing Speeds

5.8 Turbulence Intensities and High Fluctuation Regions

The same techniques used to plot velocities can be used to plot the turbulence number. Figure 5.8F1 shows an iso-velocity plot and a plot of areas of constant turbulence number for the same flow from a Curtec sprayer. This shows the relation between high turbulence number and the mean flow pattern. The relative level of turbulence intensity between two sprayers, shown by the turbulence number, can be seen in Figure 5.8F2.

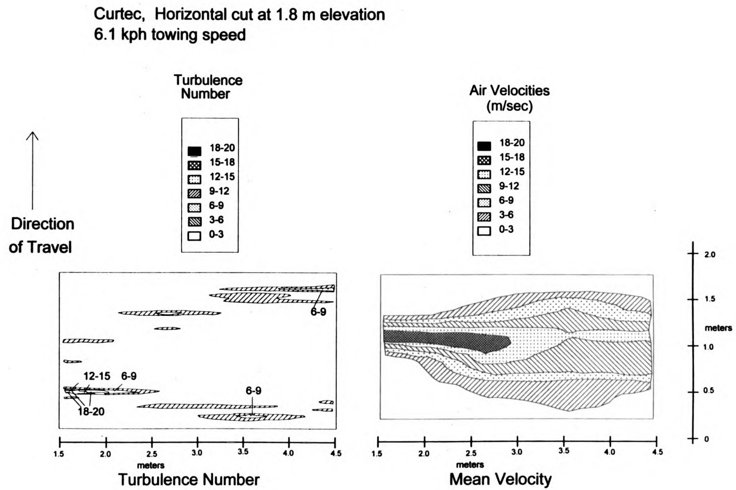

Figure 5.8F1: Iso-Velocity and Areas of Constant Turbulence Number

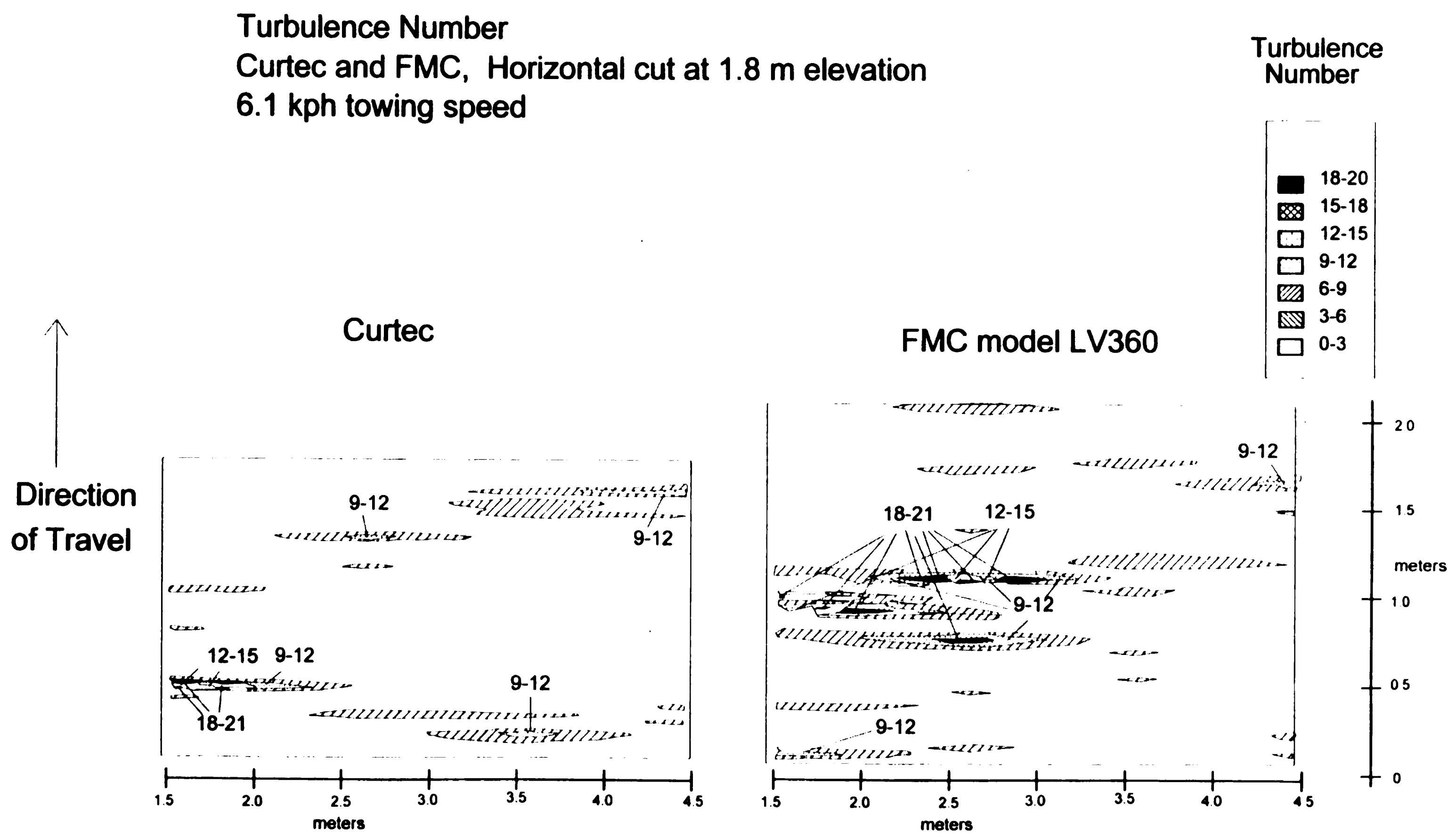

Figure 5.8F2: Turbulence Intensities for Two Different Sprayers

Chapter 6

DISCUSSION AND CONCLUSIONS

6.1 Discussion

The data in sections 5.6 to 5.8 shows that the objectives of this thesis were achieved. We were able to study the flow pattern of commercial agricultural air carrier equipment. Once the measurement equipment was designed and built the data was obtained quickly and efficiently. The measurement technique assists in understanding the basic jet flow of different machines. The data shows the effect of varying other parameters such as towing speed. The data can also reveal qualitative effects of turbulence.

Studying the plots assists in understanding the special flow patterns that different types of sprayers use to deliver chemical to trees. Figures 5.6F4 and 5.6F12 clearly show that for both conventional sprayers much of the air flow is directed almost straight up to direct chemical over the top of the tree. High velocity regions can be seen in the upper left corner of these plots. A second jet appears to be directed under the canopy to fill the tree from underneath. To a first approximation conventional sprayers appear to have a radial spray pattern but these measurements show that these machines actually have a specifically directed flow.

The tower type machine in Figure 5.6F8 shows a much more uniform pattern. It has a simple velocity gradient shown in the vertical cut plot and a broad but steady jet in the horizontal plane shown in Figure 5.6F6. The one-sided Curtec tower sprayer with cross flow fans required 18.6 kW (25 HP). The two-sided AgTec sprayer required 37kW (50 HP). While both sprayers use the same power per side, the Curtec sprayer produced much higher velocities across the measured field.

Individual characteristics of the machine design can be seen in the velocity plots. In Figure 5.6F7 velocity defects due to the gaps between the fans on the Curtec sprayer are apparent. Another characteristic that is visible in Figure 5.6F12 is the notorious LV360 "*dead spot*". There is a region of almost zero flow which has been noted by the operators of the FMC LV360. This region can be seen in the vertical views of the FMC.

The four horizontal views in Figures 5.6F2, 5.6F6 and 5.6F10 show the variation between runs. Some sprayers like the FMC in Figure 5.610 show a large variation between runs indicating instabilities on the scale of the entire jet. The Curtec shown in Figure 5.6F6 shows less variation between runs indicating a more predictable and stable jet.

Figure 5.7F1 shows a comparison of two towing speeds and the effect on two different sprayers. Some effect can be seen in the high velocities but the overall jet appears similar. A higher towing speed does slightly reduce the maximum velocity. The difference of speed is only about 20%. A more in-depth study should be undertaken to fully document the effects of speed on different sprayers. Figure 5.7F1 illustrates that this technique shows the flow pattern differences that would be required for such a study; however, for the tested case, major effects of speed were not demonstrated.

The turbulence intensity indicated by the plot of the turbulence number 5.8F1 shows expected results of a typical jet flow. On the edges of the jet, at the shear layers, there is higher turbulence fluctuations when compared to the mean. Stretching of the turbulent regions in the Z direction is an artifact of the sample resolution and the method used to analyze the data. There is a very low resolution in the Z direction. The linear interpolation routine will tend to stretch small intense region many times greater in the Z direction. The interpolation method is reasonable for mapping the mean flow because it is a smooth continuous gradient. The turbulence intensity is not necessarily a smooth gradient. There may be small spots of very high fluctuations with neighboring spots of very low intensity. This is evidenced by studying Figure 5.8F1 in the X direction where the width of the intense regions are narrow. The resolution of the field in the X direction is very high and can follow the steep gradients generated by the turbulence.

The data still shows qualitative differences between the turbulence intensity of two machines. Figure 5.8F2 shows that the machines with the greatest mean velocity across the field has fewer regions of high turbulence number. The machine with the least mean velocity, the FMC, has the more high regions of turbulence number. this would indicate that much of the energy per unit length of jet is being dissipated by the FMC machine.

6.2 Conclusions

1. The technology and techniques described in this thesis produce data for comparison of the mean air flow patterns of commercial air carrier sprayers.
2. It is possible to discern unique characteristics of the flow from different sprayer designs.

Chapter 7

SUGGESTIONS FOR FURTHER INVESTIGATION

The preceding mainly describes a tool and procedure to measure air flow patterns generated by air carrier agricultural sprayers. The areas in which this tool can be used are many. A simple and basic study would be documenting the effect of varying ground speed on the air jet. In addition, various studies could be performed to correlate the pattern of equipment in open air to the effectiveness in controlling disease; consequently, these studies could be used to guide the design of better flow patterns for new equipment.

List of References

List of References

AgTec.1990. *Sprayers, Spreaders and Application Systems.* Minnetonka, MN: Ag-Chem Equipment Co., Inc. p. 130.

Amsden, R.C. 1962. "Reducing the Evaporation of Sprays." *Agricultural Aviation,* vol. 4, pp. 88-93.

Barker, M. 1922. "On the Use of Very Small Pitot-Tubes for Measuring Wind Velocity," Proceedings, R. Soc. London Ser. A., vol. 101, p. 435.

Beyer, W.H. 1984. *CRC Standard Mathematical Tables,* 27th Edition, Boca Raton, Florida: CRC Press, Inc., p. 468.

Bird, R.B., W.E. Stewart, and E.N. Lightfoot. 1960. *Transport Phenomena,* New York: John Wiley & Sons, pp. 56-59.

Blake, W.K. 1976. *Fluid Mechanics Measurements,* New York: Hemisphere Publishing Corp., pp. 61-95.

Bukovac, M.J. 1985. "Spray Application Technology: Shortcomings and Opportunities with Special Reference to Tree Fruits," Improving Agrochemical and Fertilizer Application Technology. Agriculture Research Institute, Bethesda, MD.

Derksen, R.C. and R. L. Gray. 1995. "Deposition and air speed patterns of air-carrier apple orchard sprayers." *Transactions of the ASAE,* vol. 38 (1): pp. 5-11.

Falco, R.E. 1980. "Combined Simultaneous Flow Visualization/Hot-Wire Anemometry for the Study of Turbulent Flows," *Journal of Fluids Engineering,* vol. 102, pp. 174-175.

FMC Operators Manual. 1980. LV320 Air Sprayer Manual No. 1425089. Ripon CA: FMC Corporation. pp. B-1 and E-1.

Fox, R.D., R.D. Brazee and D.L. Reichard. 1985. "A Model Study of the Effect of Wind on Air Sprayer Jets." *Transactions of the ASAE.* vol. 28(1): pp. 83-88.

Grainger. 1996. Catalog No. 387. Chicago, IL: W.W. Grainger, p.3236.

Grafius, E., J. Hayden, G. Van Ee, and R. Ledebuhr. 1990. "Interaction Between Spray Distribution and Systemic Activity of Insecticides for Control of European Corn Borer (Lepidoptera: Pyralidae) in Peppers and Snap Peas." *J. Econ. Entomol.* vol. 83(5): pp. 2016-2021.

Hinze, J.O. 1959. *Turbulence*, New York: McGraw-Hill Book Co.

Hughes, R.R. and E.R. Gilliland. 1952. "The Mechanics of Drops," *Chemical Engineering Progress,* vol. 48(10): pp. 495-504.

Kuethe, A.M., C.Y. Chow. 1986. *Foundations of Aerodynamics.* New York: John Wiley & Sons. p. 391.

Lukshiminarayuma, B. 1982. "Three Sensor Hot Wire/Film Technique for Three-Dimensional Mean and Turbulance Flow Field Measurement." *TSI Quarterly.* vol. 8: pp. 3-13.

Marion, J.B., W.F. Hornyak. 1982. *Physics for Science and Engineering.* New York: Saunder College Publishing. pp. 253-254.

Matthews, G.A. 1982. *Pesticide Application Methods.* New York: John Wiley & Sons, p. 62.

Michigan State University, Northwest, Michigan Horticultural Experiment Station. 1993. Photo collection on display. Suttons Bay, MI.

Micro Switch. 1990. Instruction and Specification Sheet #PK 8772 4. Micro Switch. Freeport, IL.

Potter, M.C. and J.F. Foss 1982. *Fluid Mechanics.* Okemos, MI: Great Lakes Press, Inc., pp. 243-245.

Salyani, M., W.C. Hoffman. 1996. "Air and Spray Distribution from an Air-carrier Sprayer." *Applied Engineering in Agriculture.* vol.12(5): pp. 539-545.

Svensson, S.A. 1991. "Deposition and Air Velocities as Affected by Air Jet Qualities." Dissertation, Swedish University of Agricultural Sciences.

Tennekes, H., and J.L. Lumley. 1972. *A First Course in Turbulence.* Cambridge, MA: MIT Press.

Wilks, S.S. 1963. *Mathematical Statistics.* New York: John Wiley & Sons, Inc., p. 79.

Appendices

Appendix A

Appendix A

1. Droplet Dynamics Model Introduction

While an intuitive understanding of this process is easy to obtain, a simple model of droplet dynamics can help clarify the effects of various scales of flows on the transport and deposition of chemicals. Using straightforward force balances on a droplet it is possible to develop the equations of motion for a droplet in an air stream. With these equations a theoretical droplet can be "placed" into a potential flow field and numerically integrated to observe the behavior of the drop at various flow velocities and flow patterns.

2. Droplet Dynamics Model Basic Equations

To determine the path of a droplet several factors must be considered, droplet initial size and density, air flow path, droplet evaporation and initial trajectory. If a particle is moving relative to the ambient fluid, it will experience a drag force. A simple case of drag force is the terminal velocity of a particle due to gravity. The equation is known as Stokes' Law:

$$V_t = \frac{g d^2 \rho_d}{18\eta} \qquad \text{[A-E1]}$$

Where: V_t = the terminal velocity in the downward direction.

g = the gravitational acceleration.

d = the droplet diameter.

ρ_d = the droplet density.

η = the viscosity of air.

This well-known equation balances the downward force of gravity against the drag on the droplet due to the air to obtain a downward velocity. Figure AF1 shows this balance. This equation only applies to a single sized droplet in still air and does not consider evaporation that will change the droplet size as it falls.

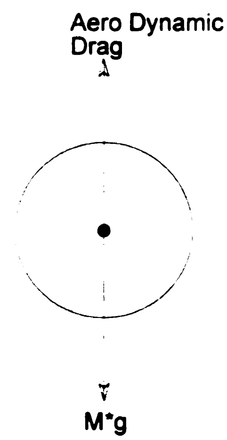

Figure AF1: Basic Force Diagram for Falling Sphere

The same logic can be applied to derive an equation that does consider all the relevant factors of a particle in a moving air stream. A particle in a moving fluid will be accelerated by a drag force due to the fluid. This acceleration will continue until the particle velocity and the fluid velocity become essentially the same. The force of accelerating the droplet is balanced by the drag of the droplet in the air.

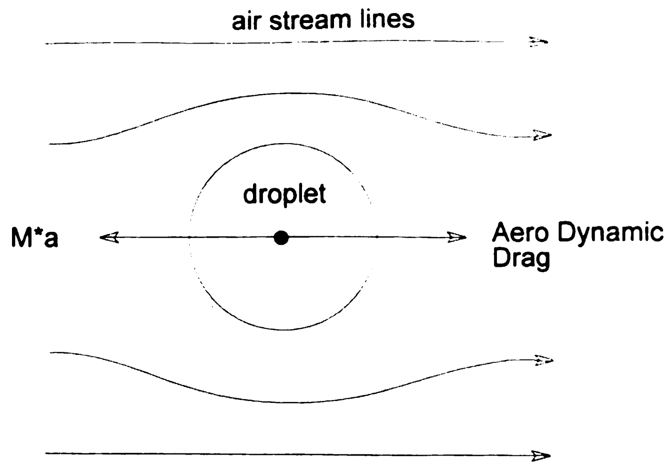

Figure AF2: Aero-Dynamic Drag Force Balance

Figure AF2 shows a diagram of this balance, in words this is the most basic mechanics equation:

The mass times the acceleration of the drop equals the drag of fluid.

Algebraically this is written:

$$\left(\rho_{drop}\frac{\pi}{6}d^{3}\right)\frac{d\vec{V}_{drop}}{dt} = 3\pi\,\mu\,d\,\vec{V}_{rel} \qquad \text{[A-E2]}$$

Where: $\vec{V}_{rel} = \vec{V}_{drop} - \vec{V}_{air}$ = relative velocity.

$\vec{V}_{drop}$ = absolute velocity of the drop.

$\vec{V}_{air}$ = absolute velocity of the air at position X.

ρ_{drop} = the droplet density.

r_{air} = the air density.

d = droplet diameter.

μ = dynamic viscosity of air.

Since this equation is in terms of absolute coordinates it is easy to add body forces of gravity and buoyancy. Then Equation A-E2 becomes:

$$(\rho_{drop}\frac{\pi}{6}d^3)\frac{d\vec{V}_{drop}}{dt} = 3\pi\mu d\vec{V}_{rel} + (\rho_{drop} - \rho_{air})\frac{\pi}{6}d^3\vec{g} \qquad \text{[A-E3]}$$

Where: $\vec{g}$ = the gravitational acceleration.

The drag force term for a sphere was first derived by Stokes. The form used here is derived by Bird, et al.(1960) and is given as Force = $3\pi\mu d\vec{V}_{rel}$. This form works well for low Reynolds number flows. At higher numbers the drag equation is traditionally given as a function of the drag coefficient C_d. Since this model is concentrating on small drops, at low relative velocities, it uses the more fundamental equation given above. This is important because the equations for the drag coefficient become undefined as the Reynolds number goes to zero. The more direct equation for the force goes to zero as the velocity goes to zero. A droplet almost at stream velocity may have extremely small relative velocity. This velocity may even change signs as the drop goes from being faster than the stream to slower. During these transitions the drag coefficient becomes undefined and the numerical integration routines can "blow up." Things do not become undefined in nature and drops really do make this transition without a problem. The use of an equation that goes to zero as the velocity goes to zero accurately reproduces what is happening.

Dividing by the droplet mass all terms become acceleration terms. This is the governing differential equation of the droplet's movement. Displaying this in terms of the position vector:

$$\frac{d^2\vec{X}}{dt^2} = \frac{18\mu}{\rho_{drop} d^2}\left(\frac{d\vec{X}}{dt} - \vec{V}_{air}(\vec{X})\right) + \vec{g} \qquad \text{[A-E4]}$$

Where: $\vec{X}$ = the absolute position vector and all other variables are the same as the preceding equations. The density of the air (ρ_{air}) was discarded because it is orders of magnitude smaller than the density of the drop.

3. The Assumption of the Drop as Sphere

The preceding analysis assumes that the droplet is a sphere. The surface tension energy of a liquid is minimized when the drop is a sphere. However, a large enough shear force due to aerodynamic drag could alter this shape. Hughes and Gilliland (1952) showed that for drops less than 2000 microns, falling in air the shape is almost completely spherical. Since most spray drops as less than 1000 microns, this assumption is very good.

4. Air Stream Lines and Path Lines of a Droplet

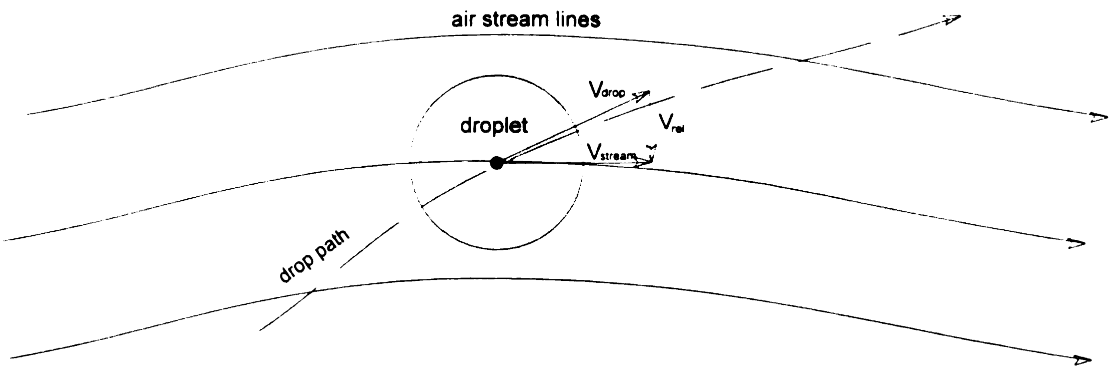

Figure AF3: Air Stream, Droplet and Relative Velocities

In a changing air velocity field the stream line of the air and the path of the particle will not be exactly parallel. In an actual air flow the particle is constantly being accelerated and decelerated due to the drag of the air. The tendency of the drop to remain approximately on the same path as the stream line is a function of three things; the droplet's mass (a function of diameter and density), the relative velocity of the particle and the air (mainly a function of the change of magnitude and direction of the air velocity), and the droplet's drag force (a function of both the diameter and relative velocity).

5. Droplet Diameter as a Function of Evaporation

In chemical application the droplet diameter is not a constant. For many liquids it will change considerably because of evaporation; therefore, the diameter becomes a function of time, liquid type and atmospheric conditions. For water drops Amsden (1962) showed that the life time of a water droplet is given by:

$$t_f = \frac{d_0^2}{80\Delta T} \qquad \text{[A-E5]}$$

and the diameter as a function of time is:

$$d(t) = \sqrt{(80\,\Delta T)\,(t_f - t)} \qquad \text{[A-E6]}$$

Where: d_0 = the initial droplet diameter.

ΔT = the wet bulb temperature - dry bulb temperature (C°).

t_f = the time when the diameter goes to zero, the end of the drop's life time.

This diameter as a function of time is substituted into equation A-E4 to obtain a more accurate determination of the particle behavior.

6. The Effect of Changing Mass on the Moving Droplet

As the droplet evaporates it loses mass, so its mass becomes a function of time. When developing a force-momentum balance on an object, the method of dealing with a changing mass is somewhat confusing. The actual method in which the mass is lost is important. First, consider a drop at rest, evaporating in air. Even though it is losing mass there is no net force because the molecules are leaving the surface with a small diffusion velocity randomly in all directions.

Next consider a drop moving in air and evaporating. Define a system that is both the drop and the vapor that has evaporated. The system will maintain a constant momentum. This momentum is:

$$M_{drop}V = (M_{drop} - M_{vapor})V + M_{vapor}V \qquad \text{[A-E7]}$$

It is obvious that since the vapor and drop still have essentially the same velocity that the net momentum is conserved. Therefore V must remain constant. This would imply that the droplet and vapor remain at the same speed. This is where the confusion arises because that is not what is observed. The vapor appears to stay in one spot while the drop moves on. Initially, it is true the vapor and drop velocities are equal. The accelerations due to the drag of the air on the drop and the vapor are orders of magnitude different. Both the drop and the vapor experience a drag force but the acceleration of the low mass vapor molecules is many times faster than the relatively high mass drop. This gives the illusion that the drop is ejecting mass at a velocity equal to the velocity of the drop in air. The relative velocity between the drop and the vapor is actually generated by external forces after the drop and vapor have separated.

Newton's Law says that for the system:

$$Force = \frac{dP}{dt} = change\ in\ momentum \qquad \text{[A-E8]}$$

The system includes the drop and the vapor; therefore, the total mass is not a function of time. Many introductory physics texts offer an equation for changing momentum of a particle in which both mass and velocity are a function of time. Marion & Hornyak (1982) state it as:

$$\frac{dP}{dt} = \frac{d}{dt}[M(t)\ V(t)] = \frac{dM(t)}{dt}V_{rel} + M(t)\frac{dV(t)}{dt} = FORCE \qquad \text{[A-E9]}$$

Where: P = total momentum.

$M(t)$ = Mass as a function of time.

$V(t)$ = Velocity as a function of time.

$dM(t)$ = the mass that is leaving.

V_{rel} = the relative velocity between the particle mass and mass that is leaving.

There is no relative velocity before outside forces act on the system. Actually there may be a small velocity due to the molecular random motion as the vapor leaves the droplet surface. But this is on the molecular scale (a diffusion velocity) and not on the much larger scale of the droplet's velocity compared to the air's velocity. The relative velocity is essentially zero, which removes the $\frac{dM}{dt}$ term from the equation. The correct equation for the force on the drop is then simply:

$$Force = M(t)\frac{dV(t)}{dt} \qquad \text{[A-E10]}$$

This is the force term that is used in this model.

7. Other Forces that May Effect the Droplet Path

Other forces may effect the droplet behavior slightly. Forces such as electro-static and gravitational forces between bodies are physically present but still orders of magnitude smaller than the inertial and drag forces. When the distance scale becomes small enough these forces become very important, they are after all the actual mechanism we call "sticking." By the time these forces become important we assume that deposition is imminent.

8. Air Flow Streamlines

The preceding analysis leads to equations to describe a droplet's path through an air velocity field. The details of an actual flow field are extremely complicated. Simple potential flow fields can be used to illustrate how a drop might behave under certain conditions. To develop equations of the velocity field around an object potential flow theory of fluid dynamics can be used. Using these velocity fields different droplets with different parameters can be "introduced" into the field and the droplets' paths can be calculated.

Potential flow is an "ideal" flow. To simulate a real flow, the complete Navier-Stoke's equations should be used. These equations are exact, but to this day they are very difficult to solve, even with the most powerful computer, for a smooth sphere in a steady flow. Calculating the flow around a leaf (including all the influences of other leaves) is not possible. The information obtained from exact calculations would not even be very beneficial. It would apply only to the exact geometry that was calculated.

Potential flow provides simple stream lines that can be generated to approximate flows that are known to exist. Various flow visualization techniques are used to determine typical flow patterns around an object. These patterns are then approximated by a potential flow equation to produce a mathematically continuous "flow field." It is possible to calculate the influence of air on a droplet in such a field.

Figure AF4 shows the stream lines around a cylinder in a steady flow field. These lines were generated by a potential flow equation.

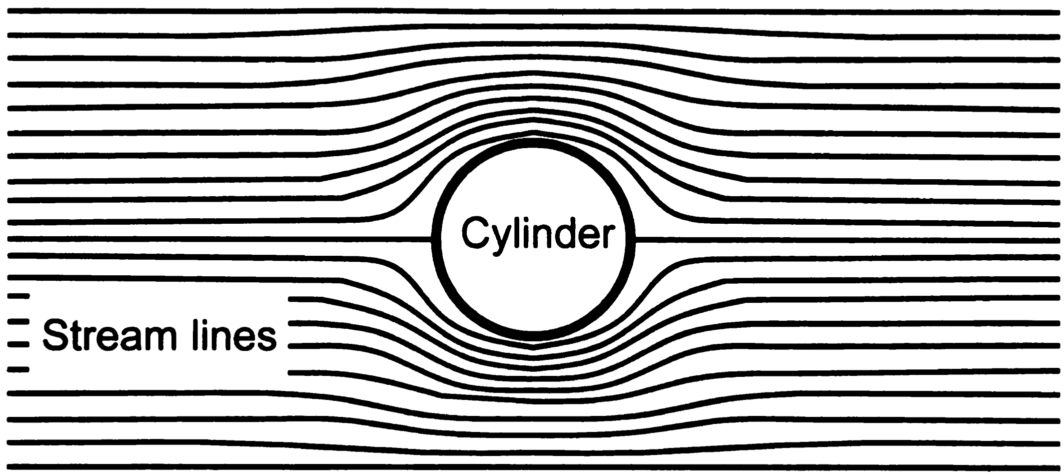

Figure AF4: Stream Lines Around a Cylinder Generated by a Potential Flow Equation

9. Discussion of the Computer Model and the Techniques Used

The differential equation A-E4 is used as the basis of the computer model. It is numerically integrated to produce the path that a drop would follow. At each time step in the integration a new; stream velocity, drop diameter, drag force and drop velocity are calculated to produce the new position. One of the more robust methods of numerical integration is the Runge-Kutta method and this is the one that is used. Many numerical integration texts discuss this method, the reference used for this model was CRC Mathematical Tables (W.H. Beyer, 1984) In this method actually each of the above parameters is calculated 4 times per time step. It is computationally intensive, but more stable than simpler techniques.

It is important that the time step is small enough to produce realistic results. The time step must be small enough that the behavior of the drop is not influenced by the step size. To test this, the number of steps is doubled and the path of the particle is plotted again. If the step size is influencing the path the new path will be different. This test was used on the paths presented in the examples.

10. Examples of the Droplet Transport Model in Simple Cases

The model is used to show some simple examples of droplet movement and transport by air currents. These examples serve to illustrate droplet behavior. When all factors are included in the model the droplets path is not always obvious. Studying these cases helps determine what scales of air flow are important to different aspects of air carrier chemical application.

Figure AF5 shows three drops in a steady 3 m/sec wind. This diagram show the effect of evaporation on actual drift distance. All three drops are released at the same height and velocity. Other investigators have reported the fall time of small drops from 3 meters. Matthews (1982) reports that the fall time for a 100 micron drop is 10.2 sec. and 40.5 sec for a 50 micron drop. These calculations are assuming no diameter change. When diameter change due to evaporation is considered the results are quite different.

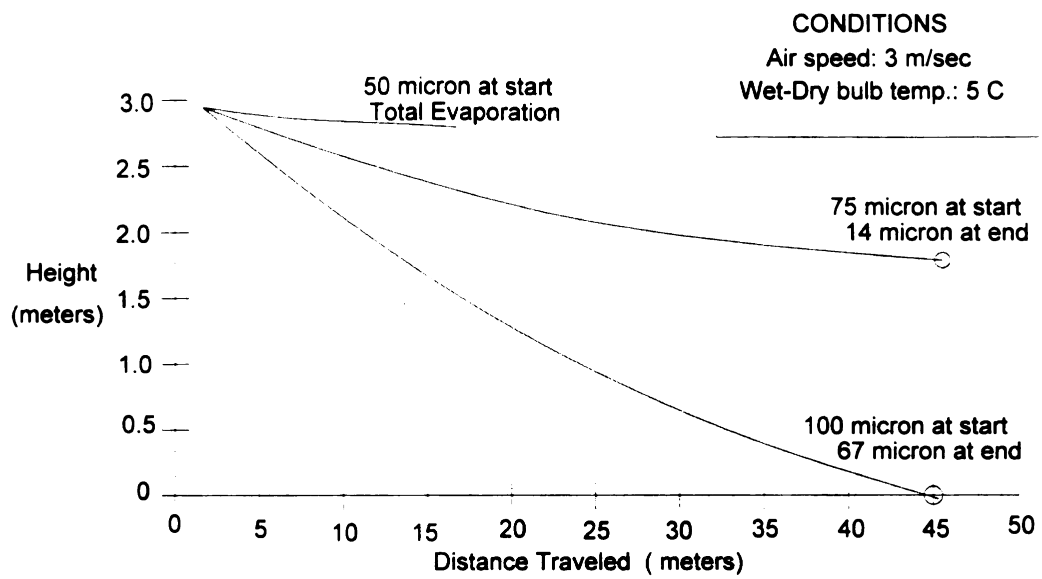

Figure AF5: Trajectories of Three Sizes of Drops in 3 m/sec Air

The 100 micron drop shown in Figure AF5 actually 13.5 seconds to reach the ground at a dry bulb-wet bulb difference of 5° C. During this extra time in the air, it drifts an additional 10 meters. The droplet is only 68 microns when it finally impacts the ground.

A 50 micron drop is reported to require 40.5 seconds to fall 3 meters. At this humidity, however, it's entire lifetime is only 6 seconds. The drop only falls 0.2 meters during its short lifetime.

The 75 micron drop's path becomes more horizontal as its diameter decreases. At the end of the plotted path it is only 14 microns.

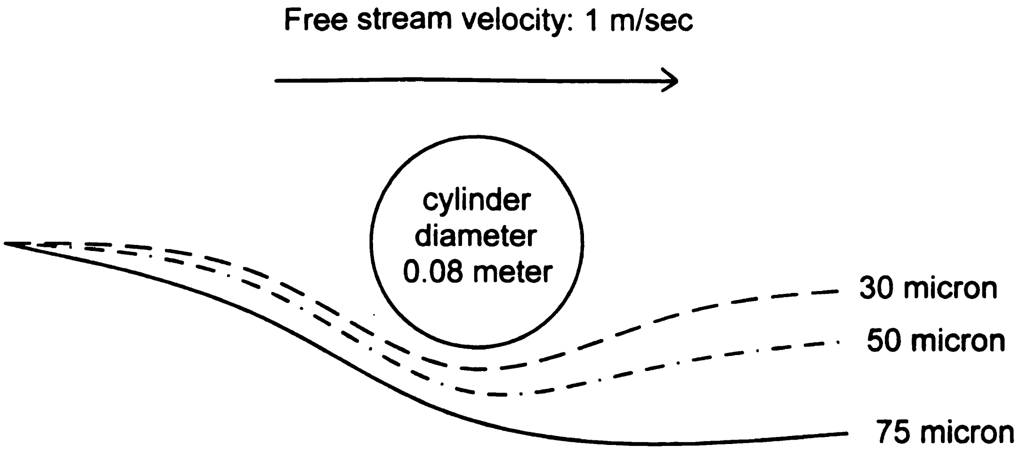

Figure AF6: Trajectories of Three Size Drops in 1 m/sec Air

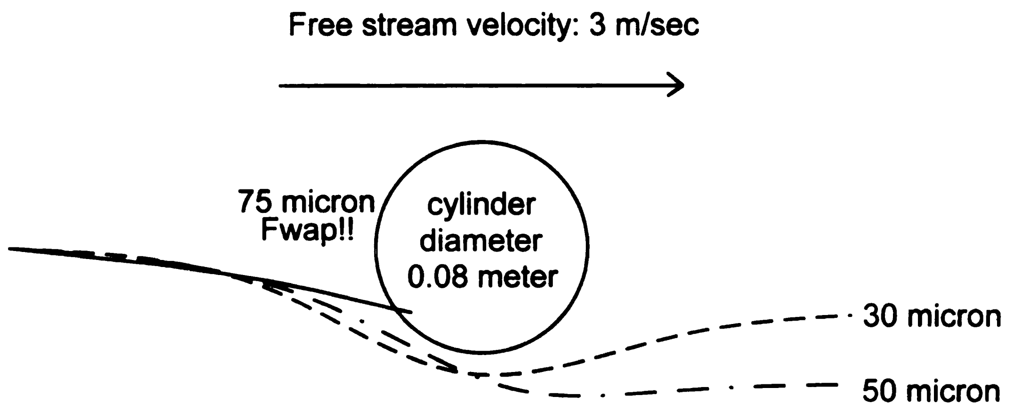

Figure AF7: Trajectories of Three Size Drops in 3 m/sec Air

Figures AF6 and AF7 show droplet paths in an air stream flowing around a cylinder. The stream lines for this flow are shown in Figure AF4. Again the droplets were released with the same initial velocity and position.

Figure AF6 shows the cylinder in a free stream velocity of 1 m/sec. All three drops can negotiate the curves in the stream lines and avoid the cylinder. Their paths, however are affected by the stream lines and their behavior is different depending on their size.

Figure AF7 shows the same drops under the same conditions except that the stream velocity is now 3 m/sec. At this velocity the stream lines are more severely affected by the cylinder and their radius of curvature is much smaller. At the higher velocity the larger drop cannot negotiate the curves and impacts the cylinder. The smallest drop still has no problem traveling around the cylinder because of its low inertia and high aerodynamic drag.

11. Using This Model to Understand What Areas of Flow Are Important to Chemical Application

In determining what methods are needed to measure air flow for air carrier spraying an understanding of the chemical transport and ultimate deposition is very important. This model illustrates the importance of many factors that are interrelated between air flow and chemical deposition. From this cursory study, it is obvious that simply delivering the air to the canopy is not the only important factor. Other important factors are the time it takes to deliver the chemical from the sprayer to the final target. Most droplets will be affected by evaporation so the actual time to deliver the drop will affect its size and therefore its deposition characteristics. The velocity at which a drop reaches the target is very important to deposition as is the amount and scale of turbulence near the target. Turbulence is a complicated and abruptly changing flow. This model shows that for high radius of curvature streamlines (as are found in turbulent flows) large droplets cannot follow the flow and are more likely to impinge near a surface.

Appendix B

Appendix B

Code and interface form for SPRAYPLOT conversion program.
Written in Visual Basic 4.0 32 bit.

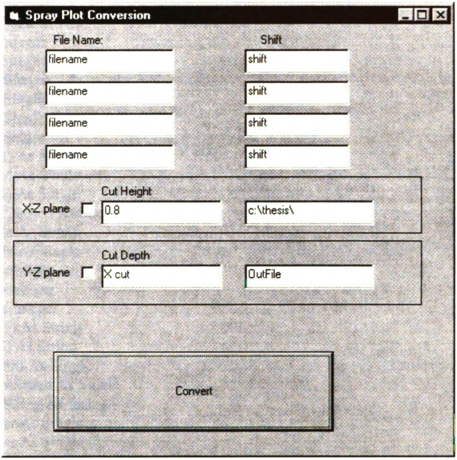

Figure BF1: Interface Form for SPRAYPLOT

```
' SPRAYPLOT
' This program converts the 4 Comma separated value files to a 3-D array
' and generates a 2-D velocity map in the specified plane.
' Written by Michael Hetherington, 8-1-96
' For the Agricultural Engineering Department at
' Michigan State University
' If you steal it without permission it would be bad!
'____________________________________________________________

'Variable Declarations
Dim i As Integer
Dim j As Integer
Dim k As Integer
Dim x As Single
Dim y As Single
Dim z As Single
Dim ddx(1) As Single
Dim ddy(1) As Single
Dim ddz(1) As Single
Dim v(16, 300, 5) As Single
Dim xScale As Single
Dim yScale As Single
Dim id As Integer
Dim jd As Integer
Dim kd As Integer
Dim ffile(5) As String
Dim file(5) As String
Dim trigShift As Single
Dim tractorSpeed As Single
Dim PrintString As String
Dim xmeter As Single
Dim ymeter As Single
Dim zmeter As Single
Dim yheight As Single

' Main Routine, this does the file reading and scaling and output.

Private Sub cmdConvert_Click()
Dim IShift(5) As Integer
frmSprayPlot.BackColor = &HC0C0C0 'reset background
file(1) = txtfilename(0).Text
file(2) = txtfilename(1).Text
file(3) = txtfilename(2).Text
file(4) = txtfilename(3).Text
```

```
IShift(1) = txtShift(0).Text
IShift(2) = txtShift(1).Text
IShift(3) = txtShift(2).Text
IShift(4) = txtShift(3).Text
'begin reading the selected files
For kk = 1 To 4
Open file(kk) For Input As #1

For i = 1 To 266

If i = 1 Then
Input #1, ffile(kk) ' remove first line of csv file
ElseIf i = 2 Then
Input #1, cow 'remove second  line of file
ElseIf i > 2 Then
' read data into array v(j,i,k)
Input #1, v(1, i, kk), v(2, i, kk), v(3, i, kk), v(4, i, kk), v(5, i, kk), v(6, i, kk), v(7, i, kk),
v(8, i, kk), v(9, i, kk), v(10, i, kk), v(11, i, kk), v(12, i, kk), v(13, i, kk), v(14, i, kk), v(15,
i, kk)
End If
If kk = 1 And i > IShift(1) Then ' deal with trigger shift, works only if Ishift is >= 0
For j = 1 To 15
v(j, i - IShift(1), kk) = v(j, i, kk)
v(j, i, kk) = 0
Next
End If
If kk = 2 And i > IShift(2) Then ' deal with trigger shift, works only if Ishift is >= 0
For j = 1 To 15
v(j, i - IShift(2), kk) = v(j, i, kk)
v(j, i, kk) = 0
Next
End If
If kk = 3 And i > IShift(3) Then ' deal with trigger shift, works only if Ishift is >= 0
For j = 1 To 15
v(j, i - IShift(3), kk) = v(j, i, kk)
v(j, i, kk) = 0
Next
End If
If kk = 4 And i > IShift(4) Then ' deal with trigger shift, works only if Ishift is >= 0
For j = 1 To 15
v(j, i - IShift(4), kk) = v(j, i, kk)
v(j, i, kk) = 0
Next
End If
```

```
Next
Close #1
Next

If chkHeight.Value = 1 Then
' make a cut at y height
ymeter = txtYCut.Text
Open txtOutFile(0) For Output As #2  'open the output file

For zzz = 1 To 100 ' 100 by 100 array
A = 0
PrintString = ""
For xxx = 1 To 100
'xmeter = 48 * (4.5 / 100)' distance of x cut for y-z plane
xmeter = xxx * (4.5 / 100) 'scale the field size
zmeter = zzz * (4.5 / 100) 'scale the field size
'ymeter = yyy * (4.5 / 100) 'scale the field size
A = MakeField(xmeter, ymeter, zmeter)
If zzz = 1 Then
PrintString = Str(A)
Else
PrintString = PrintString + "," + Str(A)

End If
Next
Print #2, PrintString
Next
Close #2
End If

If chkXcut.Value = 1 Then
' make a cut in the x direction thru forming an y-z plane.
xmeter = Val(txtXCut) * (4.5 / 100) ' distance of x cut for y-z plane
Open txtOutFile(1) For Output As #2  'open the output file

For zzz = 1 To 100   ' 100 by 100 array
A = 0
PrintString = ""
For yyy = 1 To 100

zmeter = zzz * (4.5 / 100) 'scale the field size
ymeter = yyy * (4.5 / 100) 'scale the field size
A = MakeField(xmeter, ymeter, zmeter)
If zzz = 1 Then
```

```
PrintString = Str(A)
Else
PrintString = PrintString + "," + Str(A)

End If
Next
Print #2, PrintString
Next
Close #2

End If

Beep
Beep
Beep
frmSprayPlot.BackColor = &HFF&
End Sub

' MakeField subroutine, this is the linear interpolation routine.


Public Static Function MakeField(xx As Single, yy As Single, z As Single)

x = xx / xScale
y = yy / yScale

i = Int(x)

ddx(1) = x - i
ddx(0) = 1# - ddx(1)

j = Int(y)
ddy(1) = y - j
ddy(0) = 1# - ddy(1)

k = Int(z)
If k = 0 Then k = 1
ddz(1) = z - k
ddz(0) = 1# - ddz(1)

If (i < 1) Or (i > 265) Or (j < 1) Or (j > 14) Or (z < 0.8) Or (k > 3) Then
MakeField = 0
Else
MakeField = 0
For id = 0 To 1
```

```
For jd = 0 To 1
For kd = 0 To 1
MakeField = MakeField + v(j + jd, i + id, k + kd) * ddx(id) * ddy(jd) * ddz(kd)
Next
Next
Next
End If

End Function
```

Appendix C

Appendix C

The following figures show three views of a typical spreadsheet that was generated when the data was taken. The sensor voltage data was recorded directly into Microsoft Excel. These figures are only a view of the top portion of the sheet – the data extends far below what is shown in these figures. Figure CF1 shows the raw voltages recorded at 1000 Hz. Figure CF2 shows the block reduced data and the calibration and zero constants. Figure CF3 shows the mean and fluctuating velocity data; in addition, this figure shows pertinent data for the run and a graph that instantly illustrates the mean velocity of one sensor. This graph, generated in the field during the data acquisition, assured that each run contained valid and useful data.

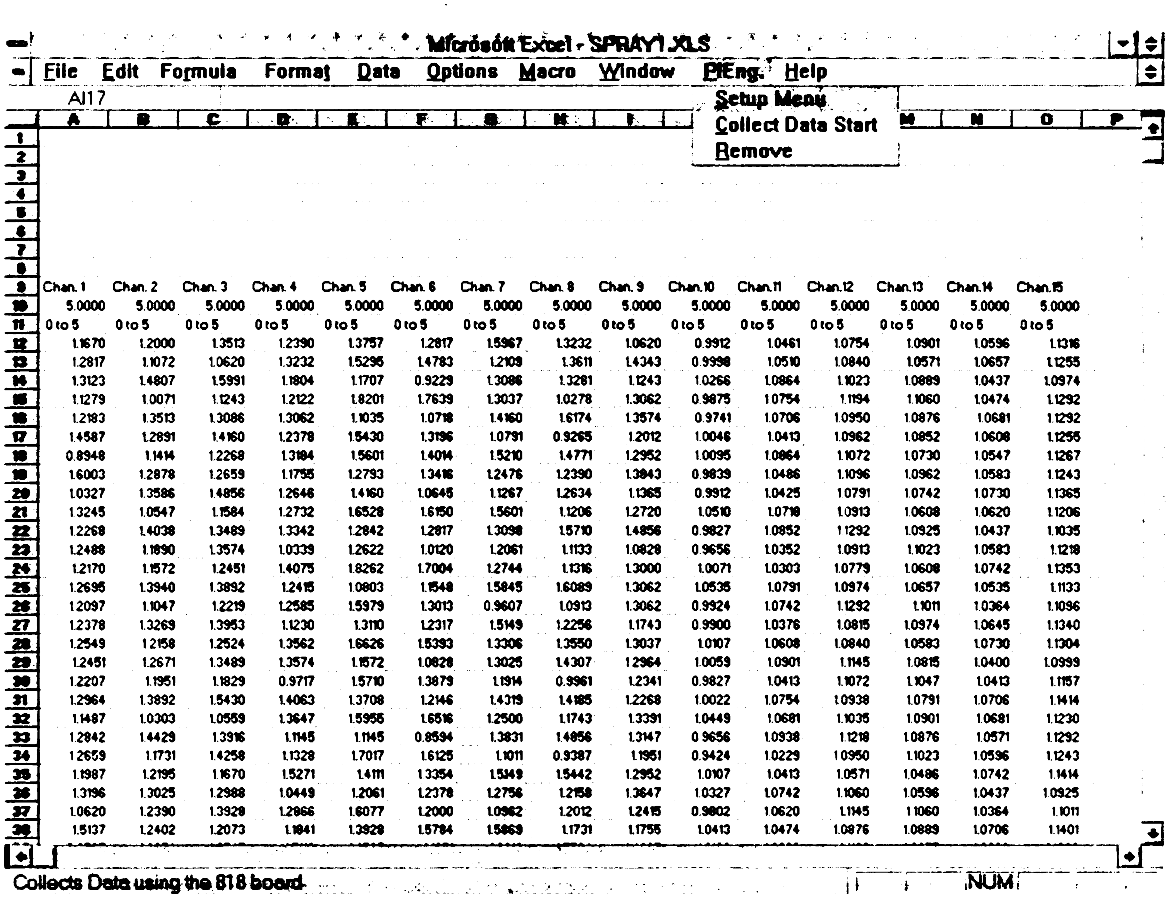

	A	B	C	D	E	F	G	H	I	J	K	L	M	N	O
9	Chan. 1	Chan. 2	Chan. 3	Chan. 4	Chan. 5	Chan. 6	Chan. 7	Chan. 8	Chan. 9	Chan. 10	Chan. 11	Chan. 12	Chan. 13	Chan. 14	Chan. 15
10	5.0000	5.0000	5.0000	5.0000	5.0000	5.0000	5.0000	5.0000	5.0000	5.0000	5.0000	5.0000	5.0000	5.0000	5.0000
11	0 to 5	0 to 5	0 to 5	0 to 5	0 to 5	0 to 5	0 to 5	0 to 5	0 to 5	0 to 5	0 to 5	0 to 5	0 to 5	0 to 5	0 to 5
12	1.1670	1.2000	1.3513	1.2390	1.3757	1.2817	1.5967	1.3232	1.0620	0.9912	1.0461	1.0754	1.0901	1.0596	1.1316
13	1.2817	1.1072	1.0620	1.3232	1.5295	1.4783	1.2109	1.3611	1.4343	0.9998	1.0510	1.0840	1.0571	1.0657	1.1255
14	1.3123	1.4807	1.5991	1.1804	1.1707	0.9229	1.3086	1.3281	1.1243	1.0266	1.0864	1.1023	1.0889	1.0437	1.0974
15	1.1279	1.0071	1.1243	1.2122	1.8201	1.7639	1.3037	1.0278	1.3062	0.9875	1.0754	1.1194	1.1060	1.0474	1.1292
16	1.2183	1.3513	1.3086	1.3062	1.1035	1.0718	1.4160	1.6174	1.3574	0.9741	1.0706	1.0950	1.0876	1.0681	1.1292
17	1.4587	1.2891	1.4160	1.2378	1.5430	1.3196	1.0791	0.9265	1.2012	1.0046	1.0413	1.0962	1.0852	1.0608	1.1255
18	0.8948	1.1414	1.2268	1.3184	1.5601	1.4014	1.5210	1.4771	1.2952	1.0095	1.0864	1.1072	1.0730	1.0547	1.1267
19	1.6003	1.2878	1.2659	1.1755	1.2793	1.3416	1.2476	1.2390	1.3843	0.9839	1.0486	1.1096	1.0962	1.0583	1.1243
20	1.0327	1.3586	1.4856	1.2646	1.4160	1.0645	1.1267	1.2634	1.1365	0.9912	1.0425	1.0791	1.0742	1.0730	1.1365
21	1.3245	1.0547	1.1584	1.2732	1.6528	1.6150	1.5601	1.1206	1.2720	1.0510	1.0718	1.0913	1.0608	1.0620	1.1206
22	1.2268	1.4038	1.3489	1.3342	1.2842	1.2817	1.3098	1.5710	1.4856	0.9827	1.0852	1.1292	1.0925	1.0437	1.1035
23	1.2488	1.1890	1.3574	1.0339	1.2622	1.0120	1.2061	1.1133	1.0828	0.9656	1.0352	1.0913	1.1023	1.0583	1.1218
24	1.2170	1.1572	1.2451	1.4075	1.8262	1.7004	1.2744	1.1316	1.3000	1.0071	1.0303	1.0779	1.0608	1.0742	1.1353
25	1.2695	1.3940	1.3892	1.2415	1.0803	1.1548	1.5845	1.6089	1.3062	1.0535	1.0791	1.0974	1.0657	1.0535	1.1133
26	1.2097	1.1047	1.2219	1.2585	1.5979	1.3013	0.9607	1.0913	1.3062	0.9924	1.0742	1.1292	1.1011	1.0364	1.1096
27	1.2378	1.3269	1.3953	1.1230	1.3110	1.2317	1.5149	1.2256	1.1743	0.9900	1.0376	1.0815	1.0974	1.0645	1.1340
28	1.2549	1.2158	1.2524	1.3562	1.6626	1.5393	1.3306	1.3550	1.3037	1.0107	1.0608	1.0840	1.0583	1.0730	1.1304
29	1.2451	1.2671	1.3489	1.3574	1.1572	1.0828	1.3025	1.4307	1.2964	1.0059	1.0901	1.1145	1.0815	1.0400	1.0999
30	1.2207	1.1951	1.1829	0.9717	1.5710	1.3879	1.1914	0.9961	1.2341	0.9827	1.0413	1.1072	1.1047	1.0413	1.1157
31	1.2964	1.3892	1.5430	1.4063	1.3708	1.2146	1.4319	1.4185	1.2268	1.0022	1.0754	1.0938	1.0791	1.0706	1.1414
32	1.1487	1.0303	1.0559	1.3647	1.5955	1.6516	1.2500	1.1743	1.3391	1.0449	1.0681	1.1035	1.0901	1.0681	1.1230
33	1.2842	1.4429	1.3916	1.1145	1.1145	0.8594	1.3831	1.4856	1.3147	0.9656	1.0938	1.1218	1.0876	1.0571	1.1292
34	1.2659	1.1731	1.4258	1.1328	1.7017	1.6125	1.1011	0.9387	1.1951	0.9424	1.0229	1.0950	1.1023	1.0596	1.1243
35	1.1987	1.2195	1.1670	1.5271	1.4111	1.3354	1.5149	1.5442	1.2952	1.0107	1.0413	1.0571	1.0486	1.0742	1.1414
36	1.3196	1.3025	1.2988	1.0449	1.2061	1.2378	1.2756	1.2158	1.3647	1.0327	1.0742	1.1060	1.0596	1.0437	1.0925
37	1.0620	1.2390	1.3928	1.2866	1.6077	1.2000	1.0962	1.2012	1.2415	0.9802	1.0620	1.1145	1.1060	1.0364	1.1011
38	1.5137	1.2402	1.2073	1.1841	1.3928	1.5784	1.5869	1.1731	1.1755	1.0413	1.0474	1.0876	1.0889	1.0706	1.1401

Figure CF1: Data Recording Spreadsheet, Raw Voltage View

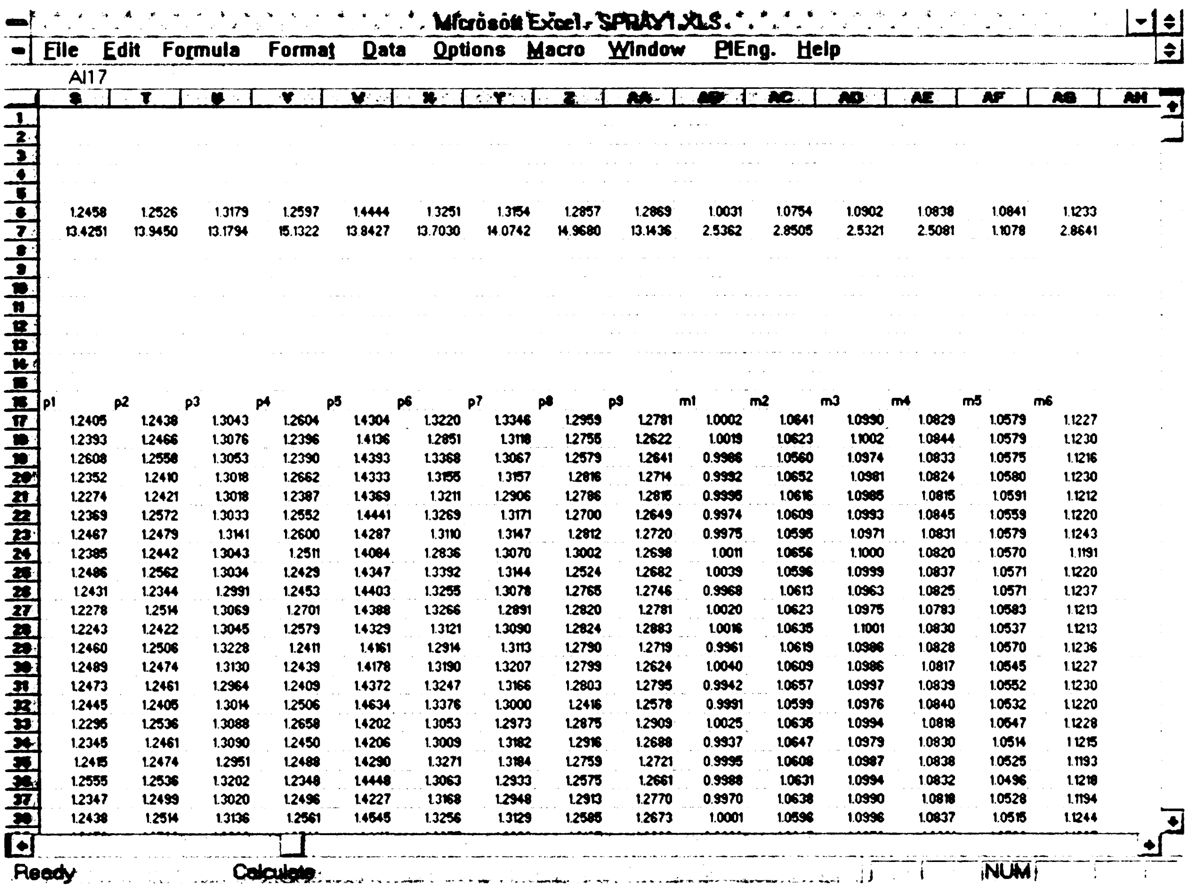

Microsoft Excel - SPRAY1.XLS
File Edit Formula Format Data Options Macro Window PIEng. Help
AI17

	S	T	U	V	W	X	Y	Z	AA	AB	AC	AD	AE	AF	AG
1															
2															
3															
4															
5															
6	1.2458	1.2526	1.3179	1.2597	1.4444	1.3251	1.3154	1.2857	1.2869	1.0031	1.0754	1.0902	1.0838	1.0841	1.1233
7	13.4251	13.9450	13.1794	15.1322	13.8427	13.7030	14.0742	14.9680	13.1436	2.5362	2.8505	2.5321	2.5081	1.1078	2.8641
8															
9															
10															
11															
12															
13															
14															
15															
16	p1	p2	p3	p4	p5	p6	p7	p8	p9	m1	m2	m3	m4	m5	m6
17	1.2405	1.2438	1.3043	1.2604	1.4304	1.3220	1.3346	1.2959	1.2781	1.0002	1.0641	1.0990	1.0829	1.0579	1.1227
18	1.2393	1.2466	1.3076	1.2396	1.4136	1.2851	1.3118	1.2755	1.2622	1.0019	1.0623	1.1002	1.0844	1.0579	1.1230
19	1.2608	1.2558	1.3053	1.2390	1.4393	1.3368	1.3067	1.2579	1.2641	0.9986	1.0560	1.0974	1.0833	1.0575	1.1216
20	1.2352	1.2410	1.3018	1.2662	1.4333	1.3155	1.3157	1.2816	1.2714	0.9992	1.0652	1.0981	1.0824	1.0580	1.1230
21	1.2274	1.2421	1.3018	1.2387	1.4369	1.3211	1.2906	1.2786	1.2816	0.9996	1.0616	1.0985	1.0815	1.0591	1.1212
22	1.2369	1.2572	1.3033	1.2552	1.4441	1.3269	1.3171	1.2700	1.2649	0.9974	1.0609	1.0993	1.0845	1.0559	1.1220
23	1.2467	1.2479	1.3141	1.2600	1.4287	1.3110	1.3147	1.2812	1.2720	0.9975	1.0595	1.0971	1.0831	1.0579	1.1243
24	1.2385	1.2442	1.3043	1.2511	1.4084	1.2836	1.3070	1.3002	1.2698	1.0011	1.0656	1.1000	1.0820	1.0570	1.1191
25	1.2486	1.2562	1.3034	1.2429	1.4347	1.3392	1.3144	1.2524	1.2682	1.0039	1.0596	1.0999	1.0837	1.0571	1.1220
26	1.2431	1.2344	1.2991	1.2453	1.4403	1.3255	1.3078	1.2765	1.2746	0.9968	1.0613	1.0963	1.0825	1.0571	1.1237
27	1.2278	1.2514	1.3069	1.2701	1.4388	1.3266	1.2891	1.2820	1.2781	1.0020	1.0623	1.0975	1.0783	1.0583	1.1213
28	1.2243	1.2422	1.3045	1.2579	1.4329	1.3121	1.3090	1.2824	1.2883	1.0016	1.0635	1.1001	1.0830	1.0537	1.1213
29	1.2460	1.2506	1.3228	1.2411	1.4161	1.2914	1.3113	1.2790	1.2719	0.9961	1.0619	1.0986	1.0828	1.0570	1.1236
30	1.2489	1.2474	1.3130	1.2439	1.4178	1.3190	1.3207	1.2799	1.2624	1.0040	1.0609	1.0986	1.0817	1.0545	1.1227
31	1.2473	1.2461	1.2964	1.2409	1.4372	1.3247	1.3166	1.2803	1.2795	0.9942	1.0657	1.0997	1.0839	1.0552	1.1230
32	1.2445	1.2405	1.3014	1.2506	1.4634	1.3376	1.3000	1.2416	1.2578	0.9991	1.0599	1.0976	1.0840	1.0532	1.1220
33	1.2295	1.2536	1.3088	1.2658	1.4202	1.3053	1.2973	1.2875	1.2909	1.0025	1.0636	1.0994	1.0818	1.0547	1.1228
34	1.2345	1.2461	1.3090	1.2450	1.4206	1.3009	1.3182	1.2916	1.2688	0.9937	1.0647	1.0979	1.0830	1.0514	1.1215
35	1.2415	1.2474	1.2951	1.2488	1.4290	1.3271	1.3184	1.2759	1.2721	0.9995	1.0608	1.0987	1.0838	1.0525	1.1193
36	1.2555	1.2536	1.3202	1.2348	1.4448	1.3063	1.2933	1.2575	1.2661	0.9988	1.0631	1.0994	1.0832	1.0496	1.1218
37	1.2347	1.2499	1.3020	1.2496	1.4227	1.3168	1.2948	1.2913	1.2770	0.9970	1.0638	1.0990	1.0818	1.0528	1.1194
38	1.2438	1.2514	1.3136	1.2561	1.4545	1.3256	1.3129	1.2585	1.2673	1.0001	1.0596	1.0996	1.0837	1.0515	1.1244

Ready Calculate NUM

Figure CF2: Data Recording Spreadsheet, Block Average Voltage View

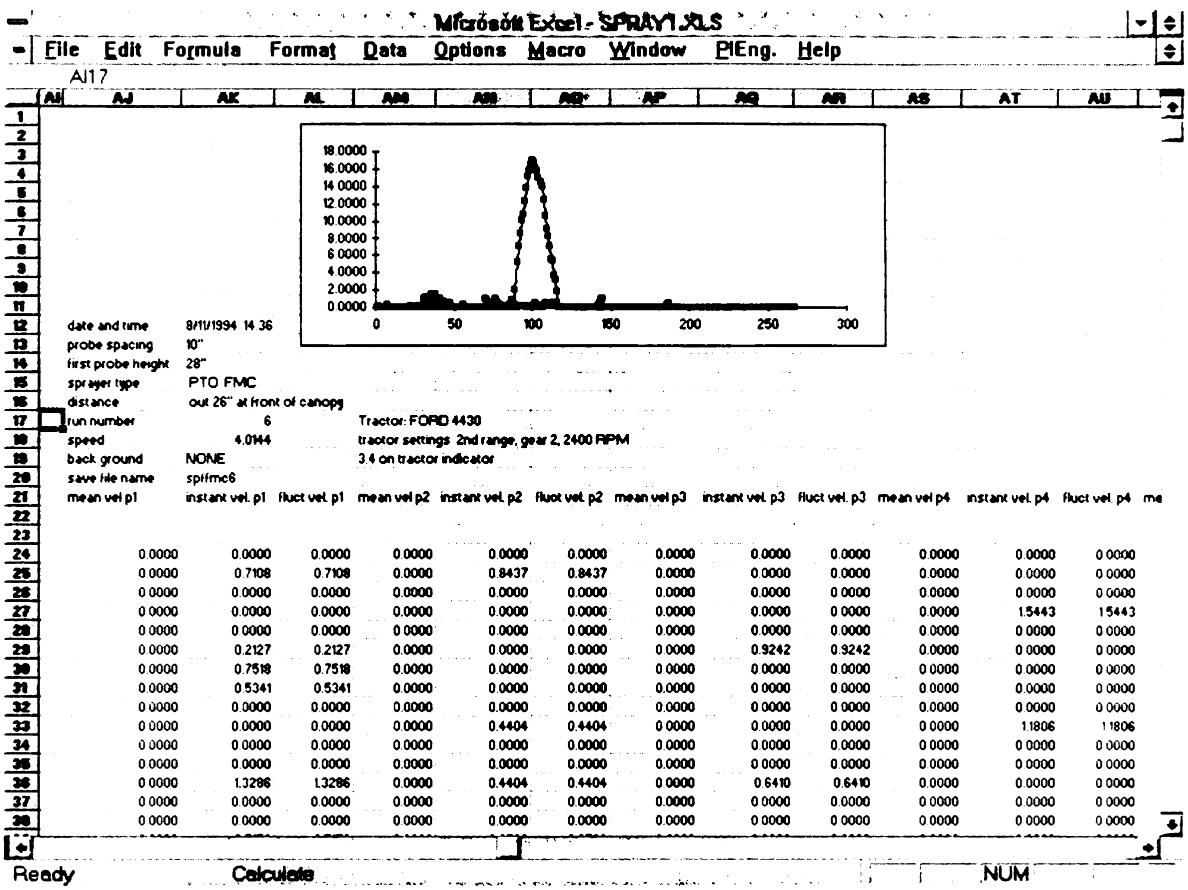

date and time	8/11/1994 14:36	
probe spacing	10"	
first probe height	28"	
sprayer type	PTO FMC	
distance	out 26" at front of canopy	
run number	6	Tractor: FORD 4430
speed	4.0144	tractor settings 2nd range, gear 2, 2400 RPM
back ground	NONE	3.4 on tractor indicator
save file name	spffmc6	

mean vel p1	instant vel. p1	fluct vel. p1	mean vel p2	instant vel. p2	fluct vel. p2	mean vel p3	instant vel. p3	fluct vel. p3	mean vel p4	instant vel. p4	fluct vel. p4	me
0.0000	0.0000	0.0000	0.0000	0.0000	0.0000	0.0000	0.0000	0.0000	0.0000	0.0000	0.0000	
0.0000	0.7108	0.7108	0.0000	0.8437	0.8437	0.0000	0.0000	0.0000	0.0000	0.0000	0.0000	
0.0000	0.0000	0.0000	0.0000	0.0000	0.0000	0.0000	0.0000	0.0000	0.0000	0.0000	0.0000	
0.0000	0.0000	0.0000	0.0000	0.0000	0.0000	0.0000	0.0000	0.0000	0.0000	1.5443	1.5443	
0.0000	0.0000	0.0000	0.0000	0.0000	0.0000	0.0000	0.0000	0.0000	0.0000	0.0000	0.0000	
0.0000	0.2127	0.2127	0.0000	0.0000	0.0000	0.0000	0.9242	0.9242	0.0000	0.0000	0.0000	
0.0000	0.7518	0.7518	0.0000	0.0000	0.0000	0.0000	0.0000	0.0000	0.0000	0.0000	0.0000	
0.0000	0.5341	0.5341	0.0000	0.0000	0.0000	0.0000	0.0000	0.0000	0.0000	0.0000	0.0000	
0.0000	0.0000	0.0000	0.0000	0.0000	0.0000	0.0000	0.0000	0.0000	0.0000	0.0000	0.0000	
0.0000	0.0000	0.0000	0.0000	0.4404	0.4404	0.0000	0.0000	0.0000	0.0000	1.1806	1.1806	
0.0000	0.0000	0.0000	0.0000	0.0000	0.0000	0.0000	0.0000	0.0000	0.0000	0.0000	0.0000	
0.0000	0.0000	0.0000	0.0000	0.0000	0.0000	0.0000	0.0000	0.0000	0.0000	0.0000	0.0000	
0.0000	1.3286	1.3286	0.0000	0.4404	0.4404	0.0000	0.6410	0.6410	0.0000	0.0000	0.0000	
0.0000	0.0000	0.0000	0.0000	0.0000	0.0000	0.0000	0.0000	0.0000	0.0000	0.0000	0.0000	
0.0000	0.0000	0.0000	0.0000	0.0000	0.0000	0.0000	0.0000	0.0000	0.0000	0.0000	0.0000	

Figure CF3: Data Recording Spreadsheet, Velocity Data View